March 2006

Chandra News

Published by the Chandra X-ray Center (CXC) Issue number 13

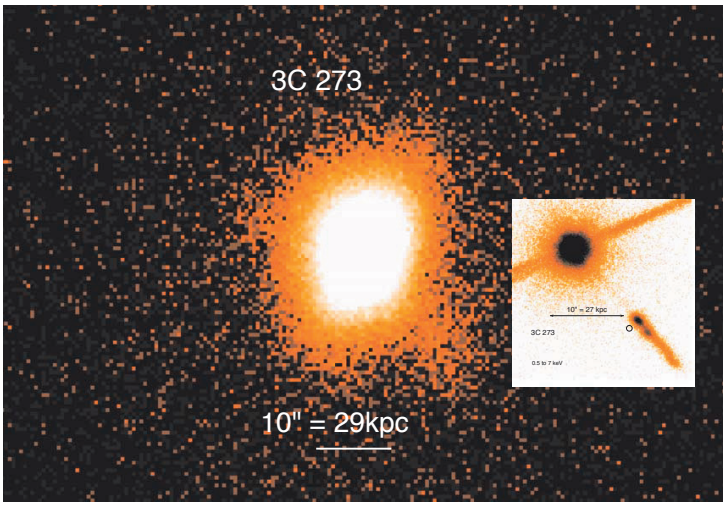

FIGURE 1: *ROSAT* (left) and *Chandra* (right insert) images of the quasar and jet in 3C 273. Both images are to the same angular scale, showing how the smaller point spread function separates the quasar from the jet which brightens about 10" from the core. The solid diagonal line in the *Chandra* image is an artifact due to the ACIS readout streak.

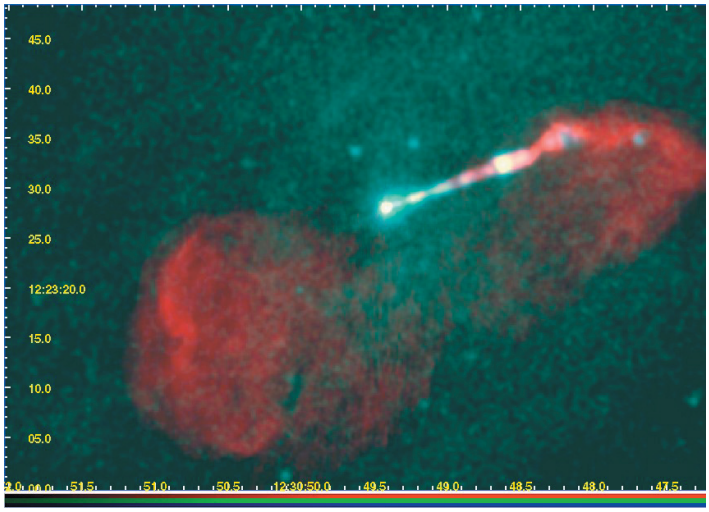

FIGURE 2: A composite image of the inner radio lobes and jet of M87. The red scale is from an 8 GHz VLA image and the green is from a 98ks 0.2 to 6keV *Chandra* image. The general green X-ray background comes from thermal X-ray emission of the hot gas pervading M87 and the Virgo cluster.

X-ray Jets: A New Field of Study

Chandra Initiates the Study of X-ray Jets

With the launch of the *Chandra* Observatory, the study of X-ray jets has developed as a new area of astronomy. Galactic X-ray jets have been studied in the symbiotic star R Aqr; the Crab, Vela, and several other pulsars; and the subset of X-ray binaries known as "microquasars" (as well as in the previously known SS 433 system). In this article we discuss only the extragalactic jets discovered by *Chandra*. These occur in Fanaroff Riley Class I and II (FR I and FR II) radio sources and quasars, covering a wide range of luminosities.

Why has the study of X-ray jets emerged just since the advent of *Chandra*? Comparison of the *ROSAT* and *Chandra* images of the nearby quasar 3C 273, shown to the same scale in Figure 1, illustrates the 100-fold increase in imaging due to the 10-fold increase in linear resolution. *Chandra* resolves the jet in one dimension, concentrates the photons along the jet, and clearly separates the jet from the quasar core that is 300 times more luminous.

The opening of this field of research was portended shortly after launch when the initial focusing adjustment using what was expected to be an unresolved quasar, PKS0637-752, showed a 10" extension to the west (Schwartz et al. 2000, Chartas et al. 2000). After immediate concerns that this was due to a problem with pointing control or the aspect solution, it was quickly realized that this 'stray' emission was associated with a radio jet, and in fact the mirror quality was so good that the jet did not compromise the use of this target to perform the focus adjustment!

What has drawn a cadre of researchers to work on X-ray jets is the situation that in spite of several decades of progress via radio observations, many of the basic questions of extragalactic jets remain unanswered. For example, we do not yet know the identity of the primary medium responsible for transferring energy from the environs of the supermassive black hole to the distant hotspots up to a Mpc away. Contenders are normal p^+/e^- plasma (either 'cold' or relativistic), pair plasma, and Poynting flux. Although we are fairly confident that jets have bulk velocities which are relativistic because of the predominant one-sidedness, we do

CONTENTS

not know if characteristic velocities $\beta = v/c$ are of order 0.5 to 0.9, or if values of β greater than 0.99 are common. Other features still hotly debated are how jets are launched, the nature of jet collimation, the internal velocity structure, the extent of entrainment and the mechanisms of deceleration.

What does the X-ray data tell us? The broad band spectral energy distribution (SED) from radio through IR and optical and to the X-rays, can help us deduce the emission mechanisms. Observations of X-rays show us a population of electrons of energy much higher or much lower (depending on the emission mechanism) than those which produce radio emission. In this article we will see how X-rays may be showing us the sites of particle acceleration, allowing observation of the low end of the relativistic electron spectrum, measuring the relativistic bulk velocities of the jets, and may even be serving as beacons to the most distant detectable activity in the early universe.

Extragalactic X-ray Jets

Many of the essential attributes of X-ray jets are illustrated in Figure 2. The non-thermal source is two sided (i.e. the two radio lobes shown in red) whereas the jet is visible on only one side, thus convincing us that relativistic beaming provides the Doppler favoritism to hide the counterjet and enhance the brightness of the jet coming towards us. Almost all of the currently known (more than 50) X-ray emitting jets are one sided. Both the unresolved nucleus of M87 (where the supermassive black hole responsible for the jets is located) and 'knot A' (the bright area near the end of the straight part of the jet) are prominent in radio and X-rays. Note that the inner part of the jet has a larger ratio of X-ray to radio brightness than regions further from the nucleus, as shown by the change from white and blue to red. Such behavior is shown by many, though not all, X-ray jets .

X-ray jets are naturally divided into two classes following the radio morphology: those from FRI radio galaxies have projected sizes generally less than 10 kpc, and those from FRII radio galaxies and quasars have X-ray jet lengths usually greater than 10 kpc. The apparent X-ray luminosities also divide with FRI's mostly $< 10^{42}$ erg s^{-1}, and quasars typically $> 10^{43}$ erg s^{-1}. Part of this dichotomy can be ascribed to selection effects from finite angular resolution and from possible differences in bulk velocities between the two types of jets. There is an ever-increasing number of jet detections from the inner segments of FRI jets. They all align well with radio features, are mostly one sided, and are of low brightness, making spectral and variability studies difficult.

One problem of immediate interest to X-ray astronomers is the uncertainty as to which non-thermal emission process is responsible for the bulk of X-ray jet emission. Although there is general agreement that synchrotron emission predominates for the low power sources (FRI), the favored, but problematic, process for quasar jets is inverse Compton (IC) emission from relativistic electrons scattering photons from the cosmic microwave background (CMB) (Tavecchio et al. 2000, Celotti et al. 2001). In the following sections, we briefly give examples of nearby FRI jets, and then discuss the higher power radio sources detected by *Chandra* surveys of radio jets.

X-rays from Low power radio jets

M87

One of the more unexpected and spectacular jet results from *Chandra* data was a large flare in the knot HST-1 0.8" from the

nucleus (Figure 3). The X-ray and optical lightcurves are shown in Figure 4, and details can be found in Harris et al. (2006). The lightcurve shows an overall increase of a factor of 50, and a rapid decay comparable to the rise time. At its peak, HST-1 was brighter than the core and the rest of the jet combined. Once we process optical and radio data already observed, we will be able to evaluate any time delays between bands, separate light travel time ('geometry') effects from electron energy loss time scales, and possibly distinguish between expansion losses and radiation losses and derive a new estimate of the average magnetic field strength. We have been exceedingly lucky to have *Chandra*'s resolution for this flare; with *Einstein, ROSAT*, or even *XMM Newton,* this event would most likely have been ascribed to the SMBH neighborhood instead of 60 to 200pc (depending on the projection angle) down the jet. The important lesson is that if one is observing an outburst from a blazer, what is seen may not be coming from a region close to the accretion disk!

Centaurus A

The X-ray jet of Cen A is the closest example of an extragalactic jet and the *Chandra* resolution of ~1 arcsec provides a spatial resolution of 17 pc, more than a factor of 4 better than for M87. As can be seen from Figure 6, the morphology is more complex than that of M87. Recent publications by Kraft et al. (2002) and Hardcastle et al. (2003) discuss the relation of the X-ray and radio morphology. Some of the radio features in the jet have moved, and some of the X-ray features have changed their intensity.

Quasar Jets

Surveys

Following the discovery of the jet in PKS 0637-752, two groups undertook short exposure (5 to 10 ks) surveys to try to assess the frequency of X-ray jet emission. Both were based on flat spectrum AGN with radio jets, so one would expect that they

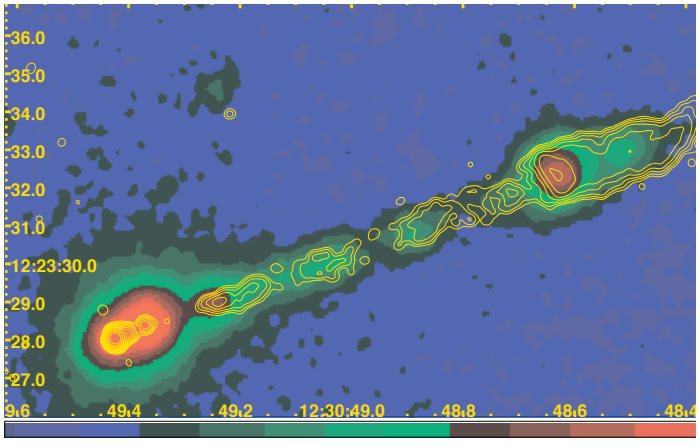

FIGURE 3: A *Chandra* image of the M87 jet, with radio contours overlaid. This image was constructed from over 20 5ks monitoring observations. The radio contours are from a VLA observation at 8 GHz; contours increase by factors of two. The nucleus is the feature to the lower left, followed by the brightest X-ray feature, HST-1. After the elongated knots D, E, & F is the bright knot A.

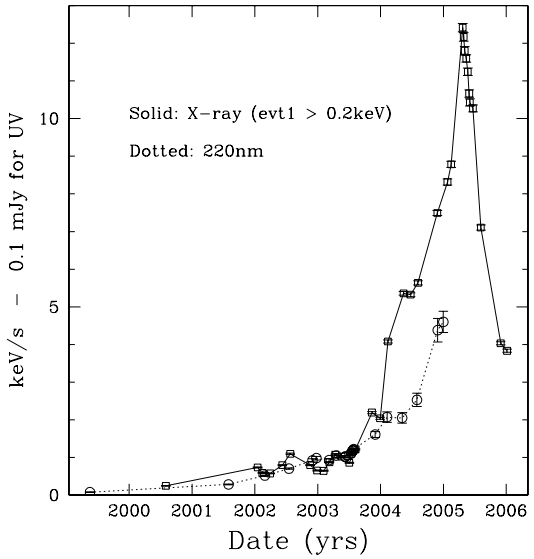

FIGURE 4: Lightcurves for the knot HST-1 in the M87 jet. The first *Chandra* observation was taken in July 2000; the most recent was 5 Jan 2006. Additional UV data from the *Hubble Space Telescope* will be available later.

are biased toward objects pointed in our direction. The team led by Rita Sambruna emphasized the coordinated search for optical emission using the *Hubble* Space Telescope (Sambruna et al.; 2002, 2004, 2006). A team led by Herman Marshall emphasized coordination with high resolution radio maps from the Australia Telescope Compact Array (Marshall et al. 2005; Gelbord et al. 2005; Schwartz et al. 2006). Both surveys detected jets at a rate of about 60%, and due to the short exposures it is reasonable to expect that the non-detections could be intrisically similar with a smaller ratio of X-ray to radio luminosity. Where X-ray emission is detected in jets, the radiated X-ray power, νf_ν, exceeds that of the radio, which is a selection effect due to the X-ray sensitivity of the short observations. Figure 5, prepared by Herman Marshall and Jonathan Gelbord, shows a montage of 20 of the 22 jets detected in their survey of 37 quasars.

A key conclusion of both studies was that the SED did not allow an extrapolation of the radio spectrum through the optical and to the X-ray, even if one includes a high energy break due to loss mechanisms. So a single population of relativistic electrons could not be producing the X-ray emission via synchrotron emission. Yet, if the region emitting the radio synchrotron radiation were anywhere near the minimum energy condition (which is nearly equivalent to equipartition of energy between magnetic fields and relativistic particles), then there were not enough electrons to produce the X-rays via inverse Compton emission off of any possible photon source. The breakthrough idea by Tavecchio et al. (2000) and Celotti et al. (2001) noted that if the jet was in relativistic motion then the CMB photon density would be enhanced in the rest frame of the jet by the square of the bulk Lorentz factor. In this case, the lowest energy X-rays detected by *Chandra* imply that the electron spectrum extends down to a minimum energy at least as low as Lorentz factors of 50, if the jet bulk motion has Lorentz factor 10, or below 500 if the jet is not

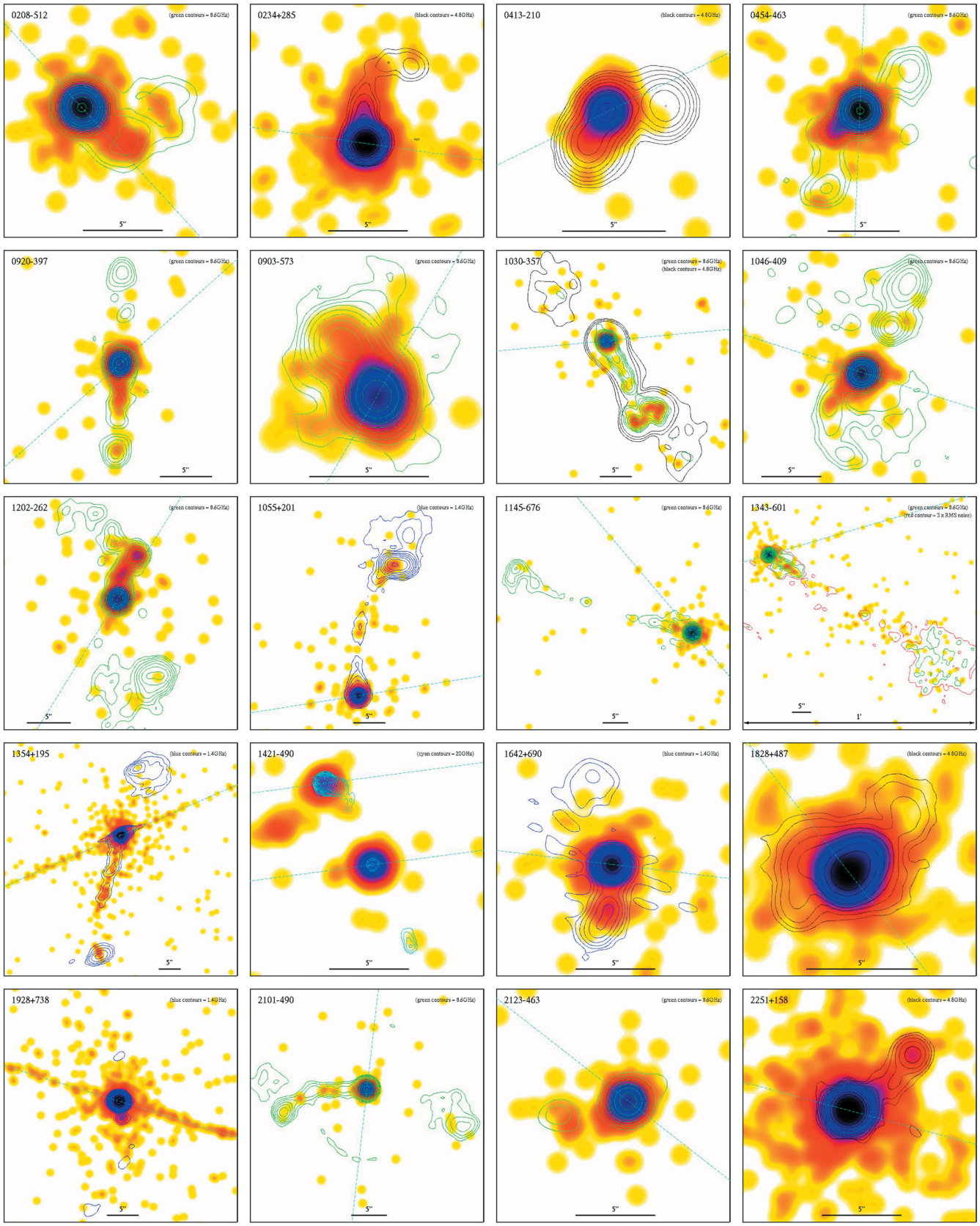

FIGURE 5: Twenty of the X-ray jets observed in the surveys by Marshall et al. False color gives the smoothed X-ray data, and the contours are the radio emission in either 1.4, 5, or 8.4 GHz. The straight dashed line shows the direction of the ACIS readout streak. The faintest yellow color corresponds to a single photon. The solid bar at the bottom gives the scale 5" in each panel.

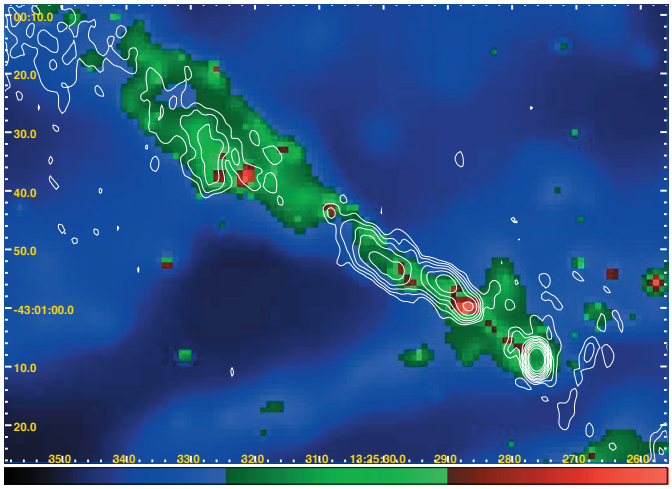

FIGURE 6: The inner portion of the jet in Centaurus A. The X-ray map was supplied by R. Kraft and is adaptively smoothed. The nuclear X-ray component is not visible because this map was made with an energy filter of 0.5-2 keV and the column density towards the core is ~10^{23} cm^{-2}. Overlayed are radio contours from the Australian Telescope Compact Array at 5 GHz, with contour levels increasing by factors of two.

in relativistic motion.

Jet Structure

With those assumptions and interpretations, one can calculate the rest frame magnetic field and the Doppler factor from spatially resolved elements along the jets. The numerical accuracy is limited by the many assumptions, including setting the Doppler factor equal to the Lorentz factor, but still restricts quantities to an allowed range of about a factor of two. Typically one finds magnetic fields in the range 5 to 25 micro-Gauss, and Doppler factors from 3 to 15. One can go on to calculate the maximum angle by which the jets could deviate from our line of sight to be in the range 4° to 20°, and hence from their measured angles on the sky we deduce their intrinsic lengths extend at least up to the order of a few million light years.

Once we know the magnetic field and relativistic velocity, we can estimate the kinetic energy flux being transported out to those millions of light years. The calculation gives fluxes of at least $10^{45.5}$ to $10^{47.5}$ ergs s^{-1}. These are often comparable to or in excess of the bolometric, isotropic radiation from the quasar itself. Such large energy transport, which must originate at the quasar black hole center, has important implications for the accretion mechanism and therefore the rate at which black holes might form in the early universe. Also, when such jets occur in clusters of galaxies they provide more than enough energy to power the cavities which have been revealed by *Chandra* observations, and to stop the cooling flow of cluster gas.

Implications of the IC mechanism

Is inverse Compton scattering on the CMB really the mechanism of X-ray jet emission? Although it is the simplest modification to producing the entire SED via synchrotron emission from a single particle population, adding only one parameter, many authors have shown that more complex sub-structure or additional electron populations, could be constructed to emit the X-rays. Indeed, in the case of the nearest object, Cen A, and the brightest quasar jet, 3C 273, there is clear evidence of spatial inhomogeneity and of independent electron populations.

Perhaps the most serious mystery for any mechanism is how the relative ratio of X-ray to radio emission is often constant, within a factor less than 2, along tens to hundreds of kpc of the jet. X-ray synchrotron emitting electrons have lifetimes at most tens of years, so there would have to be a delicate re-acceleration balance. Compton X-ray and radio synchrotron emitting electrons differ in energy by only two orders of magnitude, so in the inverse Compton CMB scenario it may be much more natural to maintain a contant emission ratio. However, that would still require the assumption that the magnetic field remains relatively constant along the jet. Basically we know that if the bulk Lorentz factor of the jet is 3 to 15, the emission of X-rays is likely to be via IC/CMB since the CMB energy density will exceed that of the magnetic field energy density. Furthermore we know the jets *are* in bulk relativistic motion from observations of one-sidedness and superluminal expansion in the AGN cores. So it may boil down to determining exactly what is the distribution of bulk Lorentz factors displayed by quasars and where does deceleration of the jet occur.

It is most exciting to pursue the IC/CMB hypothesis because of the remarkable prediction that such an X-ray jet would maintain a nearly constant surface brightness no matter how far distant it is. This is because the IC emission depends on the energy density of the CMB photons, and that density increases with redshift z as $(1+z)^4$, offsetting exactly (except for a bandwidth, or "K-correction," term) the $(1+z)^{-4}$ cosmological diminution of surface brightness. In fact, this guarantees that at some redshift, which may be modest values of 2 to 4 for jets already observed, the IC/CMB mechanism must come to dominate. Therefore, current observational capabilities would allow us to detect X-ray jets at whatever large redshift they first form!

Dan Schwartz and Dan Harris

References

Celotti, A., Ghisellini, G., & Chiaberge, M. 2001, MNRAS 321, L1
Chartas, G. et al. 2000, ApJ 542, 655
Gelbord, J. M. et al. 2005, ApJL, 632, L75
Georganopoulos, M. & Kazanas, D. 2004, ApJ 604, L81
Hardcastle, M. J. et al. 2003, ApJ, 593, 169
Harris, D. E. et al. 2006, ApJ, accepted, astro-ph/0511755
Kraft, R. P. et al. 2002, ApJ, 569, 54
Marshall, H. L. et al. 2005, ApJS, 156, 13
Sambruna, R. M. et al., 2002, ApJ, 571, 206
Sambruna, R. M. et al., 2004, ApJ, 608, 698
Sambruna, R. et al., 2006, ApJ, accepted, astro-ph/0511459
Schwartz, D. A. et al. 2000, ApJ 540, L69
Schwartz, D. A. et al. 2006, ApJ 640 in press, astro-ph/0601632
Tavecchio, F., Maraschi, L., Sambruna, R.M., & Urry, C.M. 2000, ApJL 544, L23

Project Scientist's Report

The highlight of this past year was a wonderful conference highlighting six years of observations with *Chandra* and honoring the memory of our Telescope Scientist, Leon Van Speybroeck. Project Science was especially pleased to be able to present the results of a collaborative study of the first *Chandra* field. Before the official first-light images, the *Chandra* X-Ray Observatory obtained an X-ray image of the field to which its focal plane was first exposed. Fifteen X-ray sources, the brightest being dubbed ``Leon X-1'' were detected. Based upon the analysis of the X-ray data and spectroscopy at the European Southern Observatory, we found that Leon X-1 is a Type-1 (unobscured) active galactic nucleus at a redshift z=0.3207. Leon X-1 exhibits strong Fe II emission and a broad-line Balmer decrement that is unusually flat for an AGN. The study was performed by M. C. Weisskopf, T. L. Aldcroft, R. A. Cameron, P. Gandhi, C. Foellmi, R. F. Elsner, S. K. Patel, K. Wu, and S. L. O'Dell and the results appeared in the Astrophysical Journal in February, 2006.

Project Science also continues to monitor and to support analyses of issues potentially impacting the performance of the Observatory. The following briefly summarizes the three main concerns:

1. Radiation damage to ACIS CCDs. The *Chandra* team's radiation-protection program has successfully reduced the rate of charge transfer inefficiency increase of the front-illuminated CCDs to only 2%/year. A 2005 paper (Proc. SPIE 5898, 212-223) describes the current status of radiation management.

2. Molecular contamination of ACIS. The low-energy response of the ACIS CCDs continues to drop, due to accumulation of molecular contaminants. After detailed analyses of potential risks, the *Chandra* team has indefinitely postponed a bake-out of ACIS. A major concern is that contamination-migration simulations show only a small phase space for success and a possibility of increasing the contamination on the ACIS OBF. A 2005 paper (Proc. SPIE 5898, 301-312) describes the contamination-migration modeling.

3. Thermal degradation of the spacecraft. The systematic rise in spacecraft temperatures has increasingly constrained observations. Thus, the *Chandra* team has relaxed limits on the temperature experienced by the EPHIN radiation monitor. So far, the EPHIN performance has not degraded due to higher temperatures. Nevertheless, the team has developed contingency radiation-protection plans (Proc. SPIE 5898, 212-223), should they be needed.

Martin C. Weisskopf
Chandra Project Scientist

CXC Project Manager's Report

Chandra completed its sixth year of successful scientific operations on 23 July 2005, with the spacecraft and science instruments continuing to perform in an outstanding manner. The 6-year milestone was celebrated with the "6 Years of Science with *Chandra"* symposium held in Cambridge in November. The quality and depth of the results presented at the symposium spoke to the impact that *Chandra* is having on our field. Of particular note was the number of papers that involved multiwavelength data from *Chandra, Spitzer* and *Hubble* - NASA's three Great Observatories. As we head into the 7th year of observations, it is not surprising that over-subscription rates remain very high for the *Chandra* user research programs, including the General Observer, archive research, and Directors Discretionary Time programs, and the *Chandra* Fellows program, which is now in its 8th cycle. As the mission progresses, it is clear just how important a role *Chandra* plays as NASA's prime X-ray astronomy asset.

The staff of the CXC worked hard during the last year to maintain the high standards met throughout the mission so far. Of particular note were the increasing temperatures measured in all spacecraft subsystems as the passive thermal insulation degrades due to continued exposure to radiation. The rising temperature has resulted in increasingly more complex mission planning constraints and has started to have a measurable impact on the average observing efficiency for the mission - down to 61% compared to 65% in 2004. As a result of the new thermal constraints, an increasing number of observations are now being split into multiple segments and scheduled with other observations or segments that help ensure a favorable overall thermal profile. The Flight Operations Team and the Science Operations Team are monitoring the thermal situation carefully and working to minimize the impact on the science return for the mission.

The observing program transitioned from Cycle 6 to Cycle 7 observations in December, although we expect a number of remaining Cycle 6 observations to be interleaved with Cycle 7 observations through the first quarter of the year. There were 7 schedule interruptions in the last year due to high levels of solar activity, resulting in an overall loss of about 3% of the scheduled observing time. The mission planning team responded efficiently to all the solar re-plans and minimized the science lost. Planners also responded quickly to the 13 Target Of Opportunity (TOO) observations that required schedule interruptions. Its exciting to see so many TOOs being requested following *SWIFT*'s launch in November 2004.

The spacecraft continued to operate well overall with no safe modes or major anomalies. Operational highlights included completing the earth eclipse seasons of summer 2005 and winter

2006 with nominal power and thermal performance, and passing through a lunar eclipse without incident on November 1.

The Flight Operations Team was also busy developing a number of flight software patches designed to increase the safety and science efficiency of *Chandra*. A patch was created to provide the capability to transition to Normal Sun Mode following execution of the Science Instrument safing actions (SCS 107) in response to a high radiation event. The capability ensures a favorable thermal attitude in cases when stopping the command load would violate a propulsion line thermal constraint. A second patch increased the value of the Electron Proton Helium INstrument (EPHIN) E1300 channel threshold by a factor of two. The new value will reduce the number of false triggers of the science instrument safing sequence (SCS 107) during periods of puffed-up radiation belts, and when EPHIN is at high temperature. The change will also help with mission planning by relaxing a thermal constraint. A third patch modified SCS 107 to move the Science Instrument Module (SIM) only once when SCS 107 is executed, rather than twice. The previous implementation consisted of two moves, the first to an intermediate position to allow the HRC camera door to be closed, and a second to its final HRC-S position. Because the HRC door is no longer closed during SCS 107 runs, the extra movement could be eliminated, reducing the likelihood of excessive SIM motor heating.

The science instruments also continued to operate well overall, with only a small number of minor anomalies that had little impact on the science return. ACIS experienced a recurrence of a latch-up of the threshold crossing plane circuit that affected one observation in July. The t-plane was cleared at the start of the following observation by commands that reset the ACIS Front End Processors. The reset commands are routinely included in the loads in anticipation of an occasional occurrence of this anomaly, the last having been in November 2001. ACIS also experienced an unexpected power-down of its Digital Electronics Assembly side-A. This event was thought to be due to a single event upset.

HRC experienced nominal operations with the exception of a brief episode of anomalous secondary telemetry in December. The anomalous data were seen in the engineering portion of the telemetry stream and had no impact on operations. No corruption of the X-ray event data was observed.

A number of important changes to the *Chandra* Operations Control Center ground system took place last year, including the transition in July to a direct network link to JPL (previously all mission data and communications had been routed through the GSFC closed I/ONet), and the migration to a new version of the ground system hosted on the Linux operating system. The ground team worked hard to perform the required testing to ensure a seamless transition from the old IRIX operating system and Silicon Graphics hardware. The team also prepared carefully for the 2005 leap-second and all systems handled the extra second on December 31 without difficulty.

The Science Data Processing team continued their excellent record for throughput of data, with the average time from observation to delivery of data reduced to less than 2 days. The *Chandra* archive holdings grew by 0.3 TB to 2.6 TB (compressed) during the year and now consists of 9.6 million files. A new mirror site for the archive was established at IUCAA in Pune, India.

The Data System team released software updates in support of the Cycle 7 proposal submission deadline and Peer Review, and for the Cycle 8 Call for Proposals in December. Work has also continued on preparations for the third full re-processing of the *Chandra* archive.

The Education and Public Outreach team was very active with 24 press releases, a NASA Media Telecon and 10 additional image releases. The interest in the *Chandra* web site and educational products remained at near record levels last year.

We look forward to continued smooth operations and exciting science results.

Roger Brissenden

Important Dates

Cycle 7 Observations Begin	November, 2005
Cycle 8 Call for Proposals	December 15, 2005
Cycle 8 Proposals Due	March 15, 2006
Users' Committee Meeting	April 5, 2006
Cycle 8 Peer Review	June 20-23, 2006
Cycle 8 Budgets Due	August, 2006
Cycle 8 EPO Electronic Deadline	October 20, 2006
Cycle 8 EPO Hardcopy Deadline	October 25, 2006
Chandra Fellows Symposium	October, 2006
Users' Committee Meeting	October, 2006
Cycle 8 Observations Start	November, 2006
Cycle 8 EPO Review	December, 2006
Cycle 9 Call for Proposals	December, 2006

Instruments: ACIS

Status of an ACIS Bakeout

The Chandra project decided again in July 2005 to postpone indefinitely the bakeout of the ACIS instrument. Over the past year the contamination working group evaluated new information on the expected increase in CTI due to warming the CCDs to room temperature and an expanded investigation of the uncertainties in the simulations of the migration of the contaminant during the bakeout. The MIT ACIS team conducted a new series of irradiation experiments in order to understand the on-orbit mechanism for the radiation damage better. The results of these experiments led to a refined prediction of the possible CTI increase due to warming the CCDs during the bakeout.

The MSFC project science team led an effort with considerable participation from the spacecraft team at Northrop Grumman Space Technology, the ACIS engineering team at Lockheed-Martin and MIT, the Science and Flight Operations teams in the CXC, and the ACIS science teams at MIT and PSU to develop simulation SW to model the migration of the contaminant during a bakeout and to evaluate the uncertainties in the predictions. The details of this effort can be found in O'Dell et al. 2005 SPIE, Vol. 5898, p.3010. The conclusion of this work is that given the current uncertainties, the outcome of the bakeout cannot be predicted with sufficient confidence to proceed. For the range of parameters considered in the simulations, the results of the bakeout ranged from successful to little or no effect, or perhaps to even an increase in the thickness of the contaminant. Therefore, the Chandra project has decided not to proceed with a bakeout at this time.

The CXC calibration team will continue to monitor the slow growth of the contamination layer and produce updated calibration files as necessary. The contamination working group will evaluate new information as it becomes available and reconsider the decision to bakeout if it is warranted.

Paul Plucinsky

ACIS Calibration

There are several new developments in the calibration of ACIS during the past year. As the charge transfer inefficiency (CTI) increases, we monitor gains and line shapes. Using the TGAIN formalism, we correct energies to their known values, by observing the external calibration source.

As an example of gain monitoring, we plot (Figure 7) the percent difference between fitted and actual line energies for the K-alpha lines of Mn (5.9 keV), Ti (4.5), and Al (1.49). We adjust our gain fits to try to achieve a maximum deviation of 0.3%. We meet it easily for Mn and Ti, but are pushing the limit at Al. In some other nodes for some epochs (3-month periods), the limit is exceeded, especially for middle values of CHIPY. It's not clear what is going on here physically, and it is difficult to correct this effect empirically since we have so little information on the energy dependence. Note that 0.3% is about 1 ADU at the Aluminum K line.

We noticed (Figure 8), that nodes 1 and 2 (the central two nodes) of the front-illuminated (FI) devices began to exhibit changes in their line shapes. Accordingly, we undertook to rederive the CTI trap maps, which are used by acis_process_events for correcting (some of) the effects of CTI, using external cal source data from the year starting August 2004. It also proved necessary to implement a finer grid of chip regions for which TGAIN is calibrated, from the old standard of 32 x 256 pixel

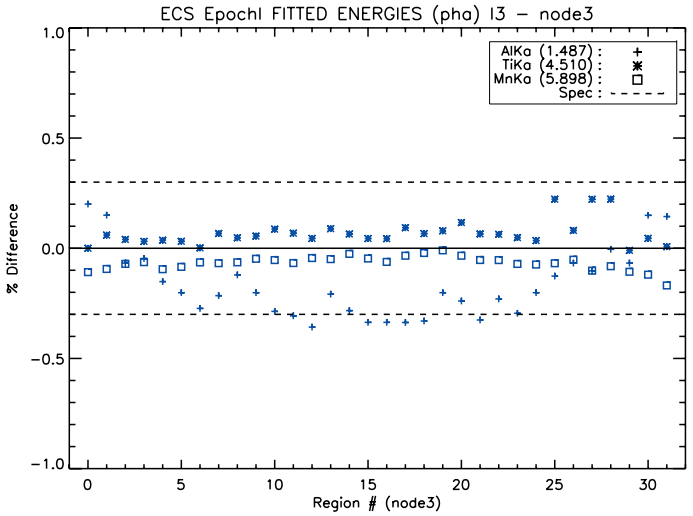

FIGURE 7: Percent difference between fitted and actual line energies for Mn, Ti and Al Kα lines in the external calibration source, as functions of CHIPY (binned in units of 32 pixels). The spec is ~0.3%, and is plotted as dashed lines. Courtesy Joe DePasquale.

regions to 32 x 32 pixel regions.

What's happening here is a gain droop for a roughly 30 columns near the center of the device (Figure 9). This electrical effect is understood, but it appears to the user as extra CTI for these columns.

The CALDB with these second-epoch trap map files, and response products to match, was released in November 2005.

Herman Marshall's work with a number of faint continuum sources (Blazars) with HETG data shows that there is a feature in the system throughput near the Si K edge at 1840 eV. This 6% effect may be the result of several effects, all due to the fact that the mean free path of photons in the device is much shorter just hardward of the edge than on the softer side. Events convert into electron clouds closer to the surface, and fluorescent photons and even electrons may not be collected. We are looking at these effects to see if they add up to the required correction.

We are also looking into implementing CTI correction for back-illuminated (BI) devices. This is somewhat trickier than for the FI devices, since there is serial CTI in addition to parallel. A new revision of acis_process_events and the associated calibration files is expected in the spring of 2006. Also anticipated in 2006 is CTI correction for FI devices at a temperature of -110 C (which was the operating temperature of ACIS from September 1999 through January 2000). We will also work on BI CTI correction at -110, but the release date is less clear.

Dick Edgar

ACIS Science: Chandra Observations of the Massive Stellar Cluster Trumpler 14 in Carina

Most stars are born in massive star-forming regions (MSFRs); the most massive stars live out their short lives in this environment and eventually transform it when they explode as supernovae. The *Chandra X-ray Observatory* is providing remarkable new views of these complex regions, revealing all stages in the life cycle of high-mass stars and their effects on their surroundings.

The Great Nebula in Carina is a remarkably rich star-forming complex at the edge of a giant molecular cloud, at a distance of ~2.3 kpc. It contains many open clusters with at least 64 O stars, several Wolf-Rayet stars, and the luminous blue variable Eta Carinae. The presence of these evolved stars may indicate past supernovae, although no well-defined remnant has ever been seen.

Tr 14 is a young (~1 My), compact OB cluster near the center of the Carina complex, containing at least 30 O and early B stars. At its center is HD 93129AB, a very early-type (O2I - O3.5V) binary. Tr 14 is probably at nearly the same distance as its neighboring, even richer cluster Trumpler 16 (Tr 16), host of Eta Carinae. These two clusters contain the highest concentration of O3 stars known in the Galaxy; their ionizing flux and winds may be fueling a bipolar superbubble.

An *Einstein* X-ray study of the Carina star-forming complex detected ~30 point sources, mostly individual high-mass stars and the collective emission from unresolved cluster cores. Also

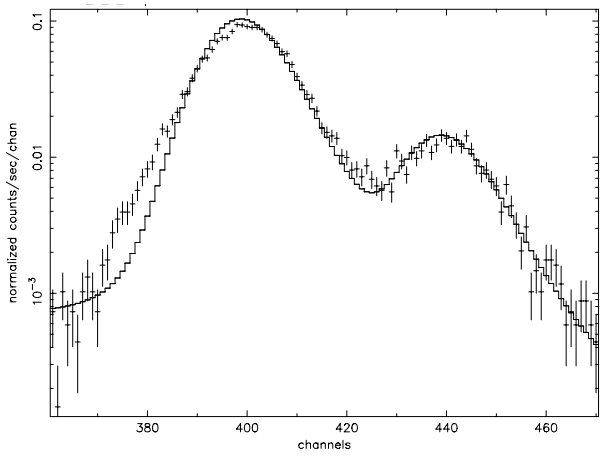

FIGURE 8: Mn K-alpha and K-beta lines, integrated over node 1 of the S2 chip. The solid stepped line is the Spring 2000 data, while the data points are Spring 2005 data. Note the change in the line shape.
Courtesy Alexey Vikhlinin.

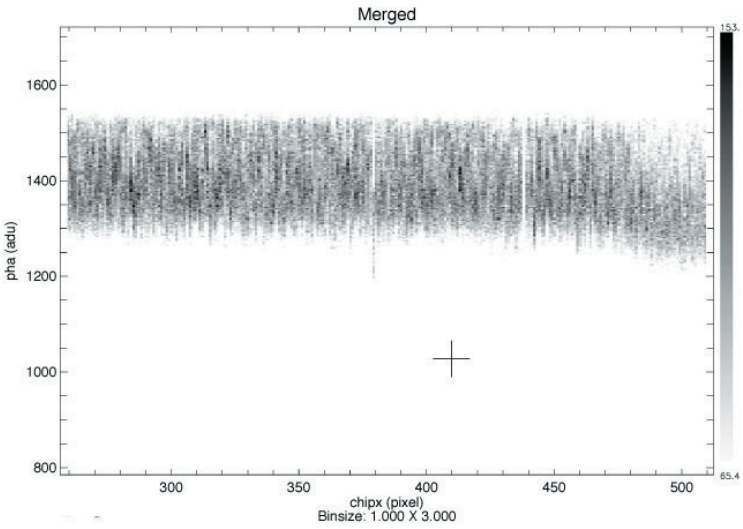

FIGURE 9: A scatter plot pulse height vs column number for the Mn K-alpha line on S2c1 from August 2004--July 2005. Note the decrease in the mean pulse height for columns above ~470.

seen was diffuse emission pervading the entire region, possibly due to O star winds. Based on experience with *Chandra*, we now know that thousands of the lower-mass stars in these young clusters were likely to be contributing to the diffuse flux seen in the *Einstein* data. A major goal of our *Chandra* observation was to resolve out a significant fraction of this point source emission so that a better determination of the spatial and spectral characteristics of the diffuse component can be made, giving clues to its origins.

Our 57-ksec ACIS-I observation of Tr 14 with HD 93129AB at the aimpoint revealed ~1600 point sources and showed that extensive soft diffuse emission remains; the off-axis S2 and S3 CCDs also show very bright diffuse emission. Based on other *Chandra* observations of stellar clusters, we expect ~90% of these sources to be stellar members of Tr 14 and Tr 16 rather than unrelated foreground stars or background AGN. Since the two components of HD 93129AB are resolved in the ACIS data, we can see that they have very different spectra; both stars show the ~0.5 keV thermal plasma typical of O stars, but HD 93129A also requires a second, much harder thermal plasma component, with kT =2.6 keV. We find that the O3.5V star HD 93250 in Tr 16 requires a similar 2-component plasma with a hard component of kT = 3.3 keV, while the O3.5V star HD 93128 in Tr 14 shows a single soft component. Similar hard emission has been seen in other *Chandra* and XMM observations of massive stars; it may be due to colliding winds in close binary systems or to complex magnetic field interactions.

Soft diffuse X-ray emission pervades the Tr 14 H II region and is resolved from the point source population; part of it is most likely from the fast O-star winds that thermalize and shock the surrounding media. Its asymmetric spatial distribution is due in part to the Carina I molecular cloud lying just west of Tr 14. The brighter diffuse emission to the southeast of Tr 14 is mysterious. The part on the I3 chip is intrinsically brighter and more absorbed than the bright swath seen on the S3 CCD, although its apparent surface brightness is reduced due to absorption. This bright swath on S3 is far from any of Carina's massive clusters and its spectral fit requires no absorbing column. Both the I3 and S3 diffuse emission are well-fit by a thermal plasma with kT ~0.6 keV, but the I3 emission requires an additional component with comparable normalization at kT ~ 0.3 keV. The S3 fit requires high abundances of Ne and Fe. The spatial and spectral characteristics of this diffuse X-ray emission provide evidence that it may be the signature of an old cavity supernova remnant from a star that exploded inside the Carina superbubble.

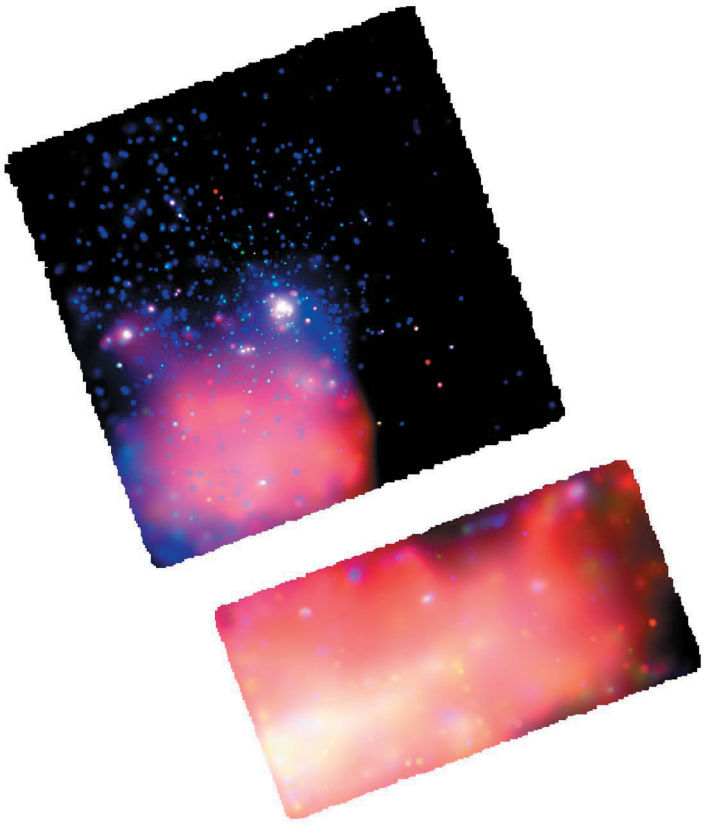

FIGURE 10: Trumpler 14 in Carina, 57 ksec ACIS-I. Red = 350-790 eV; green = 790-970 eV; blue = 970-1650 eV.

This article was excerpted from:

Townsley, L. K., Broos, P. S., Feigelson, E. D., & Garmire, G. P. 2005, IAU Symposium, 227, 297.

Additional references can be found in that article.

Leisa Townsley
Penn State University

Instruments: HRC

Status of Flight Instrument

The HRC continues to operate smoothly with no major problems or anomalies. Ongoing monitoring of the HRC QE (via observation of AR Lac) and UV sensitivity (via observations of Vega) indicates no change in either. As noted in our previous newsletter, there was some concern that the increased radiation dose received by the HRC may have weakened the polyimide in the UVIS. Such weakening would manifest itself as increased UV sensitivity. The HRC gain continues to slowly drop due to the extraction of charge by X-ray and particle events. This effect is still small and any necessary increase in the MCP high voltage to recover the detector gain is several years away.

The secondary science telemetry of several HRC observations made in mid-December, 2005 was corrupted for reasons yet unknown. This problem has not been observed in any observation since, including the 500 ks observation of 47 Tuc at the end of the year. The instrument team, the CXC, and the Chandra FOT are continuing to investigate this problem. It is currently thought that this may be a thermal issue unrelated to the HRC.

The HRC laboratory was moved from Porter Square in Cambridge, MA, to new facilities in the Cambridge Discovery Park (near the Alewife T station) in Nov/Dec 2005. The instrument team is in the process of re-assembling the laboratory to support on-going HRC operations.

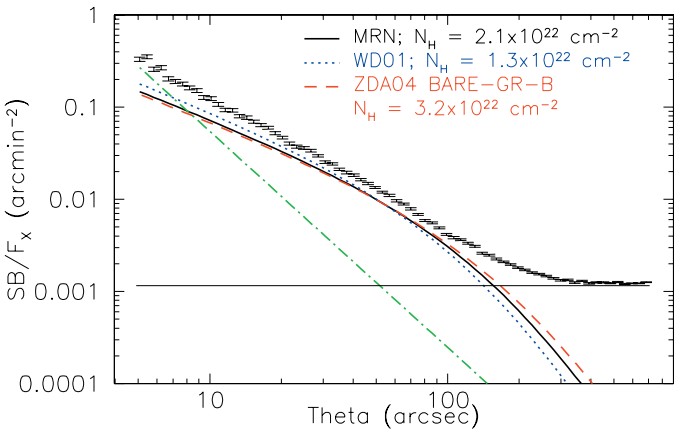

FIGURE 11: Normalized radial surface brightness profile of HRC-I observation of GX 13+1 (including error bars). The green line is the *Chandra* PSF, the solid black line is the background level, and the other three curves are scattering from dust grain models described in the text.

Science Highlights

The HRC has been used to make a wide range of scientific investigations over the past year, including deep observations of the globular cluster 47 Tuc, M31*, and the nucleus of NGC 5548. Here we present preliminary results from one of the HRC observations of the past year, a study of the small angle dust-scattering halo around GX 13+1.

Smith, Edgar & Shafer (2002) analyzed the X-ray halo seen by ACIS around GX13+1 between 50" to 600", finding that the data fit both the Mathis, Rumpl & Nordsieck (1977; MRN) and Weingartner & Draine (2001; WD01) grain distributions, although with very different best-fit N_H values. A low N_H was found for the WD01 model, along with slightly inferior fits compared to MRN. Draine (2003) noted that these oddly low N_H values found for the WD01 above might be explained by dust near the source, to which the ACIS observations were insensitive. Xiang et al. (2005) analyzed the halo of GX13+1 along with 16 other sources from the zero-order HETG image. In all cases, they found that the majority of dust along the line of sight is very near the source, and proposed that all or most XRBs are surrounded by molecular clouds. To test this, they obtained 9 ksec of HRC-I data (without a grating) on Feb 8, 2005. These data allowed them to measure the halo (albeit without any spectral information) for three of the sources; this is the first time an X-ray halo has been measured this close to a source. (Figure 11) Since the GX13+1s spectrum is variable, they also obtained simultaneous RXTE data to measure it. They also used HRC-I Chart simulations to determine the PSF, the same tool used to calibrate the *Chandra* PSF. The initial analysis simply fit a smooth dust distribution using a flux-weighted halo model. Although none of the fits are formally acceptable (χ^2 = 3.4-6.5), they show no sign of significant dust near the source. They were therefore able to confirm the results from the ACIS observation, with the WD01 model again showing the worst fit along with a low column density. However, they note this result crucially depends on the *Chandra* PSF (the green curve) and the spectral model of the source, so additional work is needed.

Ralph Kraft and Almus Kenter

References

Draine, B. T., and Lee, H. M. 1984, Ap. J., 285, 89.

Mathis, J. S., Rumpl, W., and Nordsieck, K. H. 1977, Ap. J. 217, 425 (MRN)

Smith, R. K., Edgar, R. J., and Shafer, R. J. 2002, ApJ, 581, 562

Weingartner, J. C., and Draine, B. T. 2001, Ap. J., 548, 296 (WD)

Xiang, J., Zhang, S. N., and Yao, Y. 2005, Ap. J., 628, 769.

Instruments: HETG

HETG Calibration

The HETG spectrometer continues to provide high-quality dispersed spectra with stable characteristics. In the past year, progress was made on the effective area calibration of the HETGS by including an update to the HEG and MEG efficiencies and a correction for the HRMA's Ir M-edge response. These updates were released on 15 December 2005 in the CALDB version 3.2.1. The efficiency changes bring the HEG and MEG spectra into agreement: the error between them was apportioned to the HEG below and the MEG above a cross-over point of 1 keV. Using these updated calibration products, fractional residuals in spectral fits should now be less than 5% from 0.5 to 8 keV - provided that one is fitting the "real" source model! The major remaining degree of calibration freedom, the absolute effective area, is being studied through on-going cross-calibration, in particular with the XMM-Newton instruments and the RXTE PCA.

With these calibration improvements, the six years of HETGS data form a unique and coherent spectral resource. We're also entering a new era of HETGS calibration focussing more on calibration's effects on science conclusions, e.g., along the lines begun in the special session on "Incorporating Calibration Uncertainties into Data Analysis" at the Chandra 2005 Calibration Workshop [0]. As always, up-to-date HETG calibration status and details are available on the web [1].

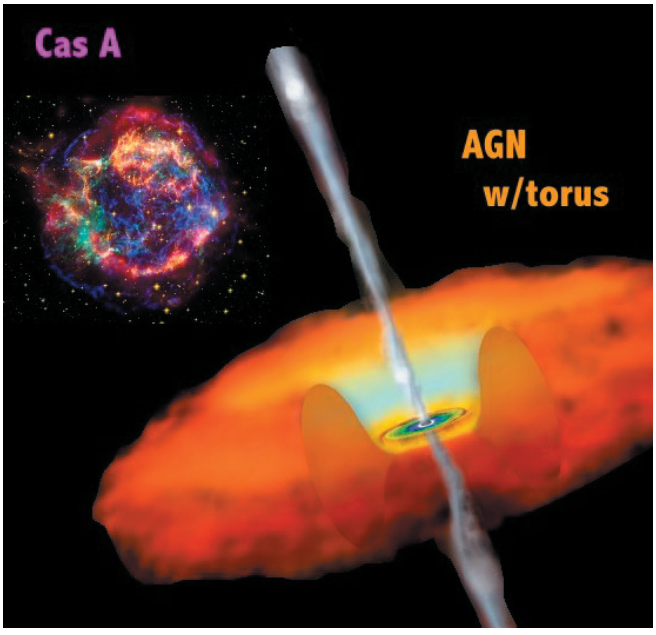

FIGURE 12: An illustration of a generic Seyfert AGN. At the distance of NGC 3783 this image would subtend one-tenth of an arc second on a side. Interestingly, the AGN's physical scale is of the same order as that of Cas A, as shown.

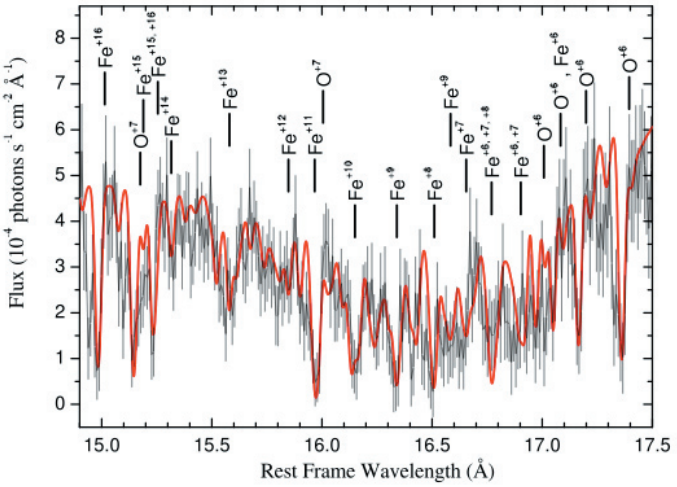

FIGURE 13: HETGS spectrum of NGC 3783 in the Fe-M unresolved transition array (UTA) region fitted with a detailed ion-by-ion model, red line. (From Holczer et al., Fig.2)

We note for HETG fan[atic]s that the infamous "HETG paper" has been published: Canizares et al. 2005 [2]; it includes many gory details of the design, fabrication, ground and flight calibration of the HETG. Although not required reading for the general observer it is a useful reference and may give future instrument builders a hint of what they're getting into.

HETG Science: The AGN NGC 3783

The object NGC 3783, an active galactic nucleus (AGN), is thought to harbor a 30 million solar-mass black hole which is surrounded by an accretion disk, out flowing ionized material, and

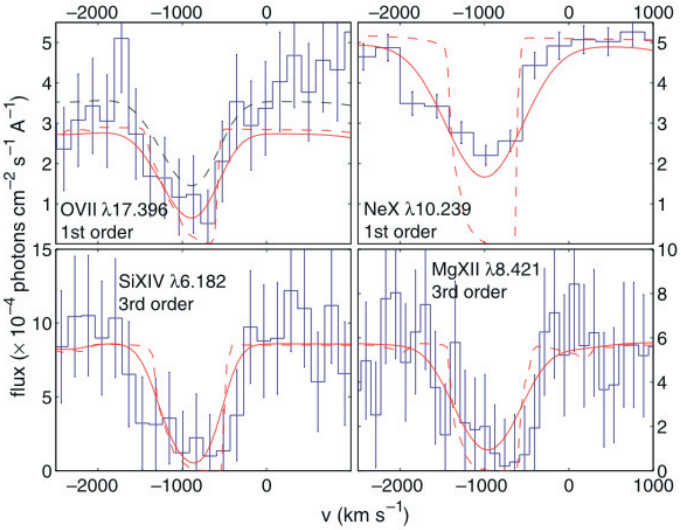

FIGURE 14: Best-fit model (solid lines) to MEG and HEG first-order and MEG third-order absorption-line profiles. The asymmetric model line shape before instrumental convolution is shown as well (dashed.) (From Chelouche et al., Fig.11)

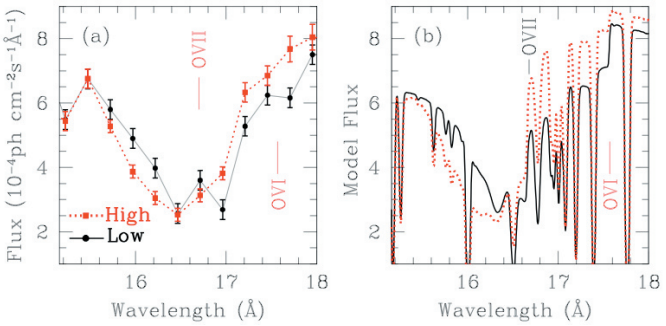

FIGURE 15: (a) HETGS spectra of NGC 3783 in the UTA region for spectrally-identified "low" and "high" states. (b) Plotted here are spectra from a photoionization model for a nominal central source flux and for a flux change by a factor of 2. The model change is in agreement with the low-high state difference seen in (a). (From Krongold et al., Fig.1(a)(b))

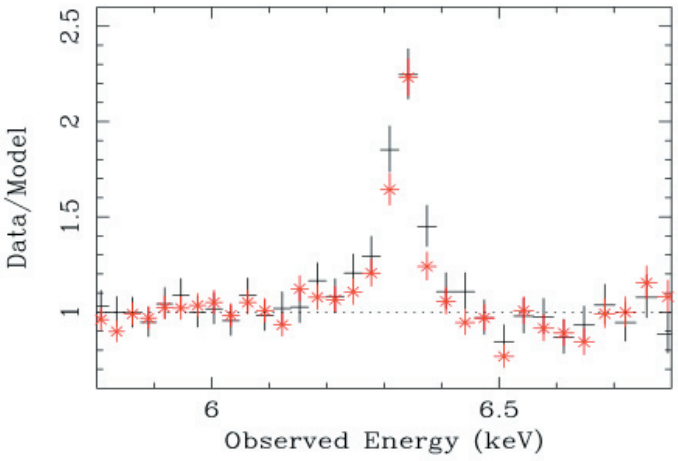

FIGURE 16: Ratios of the HEG spectrum to a simple power-law continuum model. The Fe-K emission line is shown for data separated into two states and hints at a slightly broader core in one set ("+" symbols) than in the other ("*" symbols.) (From Yaqoob et al., Fig.5)

an obscuring torus; Figure 12 illustrates the geometry. If viewed at the orientation of this illustration, the central source would be obscured by the torus and this would be classified as a Seyfert 2. NGC 3783, in contrast, is a Seyfert 1 where our viewing angle is above/below the torus and lets us see directly to the bright, central source. In terms of its physical size, the inner diameter of the torus is of the order of parsecs, roughly the same size as the Cas A supernova remanant in our Galaxy. Located about ten thousand times further away from us than Cas A, NGC 3783 appears as an unresolved point source to the *Chandra* telescope and so its spectrum is the main source of detailed information.

Back in the years 2000 and 2001, HETGS observations totaling 900 ks were dedicated to NGC 3783, a cycle 1 GTO (PI: G. Garmire) and a cycle 2 GO (PI: I. George.) The observations were carried out and the spectra were analyzed and published in a timely fashion [3,4]. The bright continuum spectrum emitted by the central source was seen to contain many absorbtion lines, generally blue-shifted from the galaxy's rest frame at z=0.00976. These are interpreted as being due to outflowing gas along the line of sight. Much of the absorbtion is not from cold, neutral atoms but from ionized atoms, i.e., a "warm absorber".

Even with the extensive analysis given, this data set is not depleted: during the past year there have been at least 5 further papers explicitly making use of these HETGS data to carry out new analyses [5,6,7,8,9]. Example spectra and highlights from these papers are shown in Figures 13 through 17. Clearly, these are spectra that tell a story - and it's still in translation.

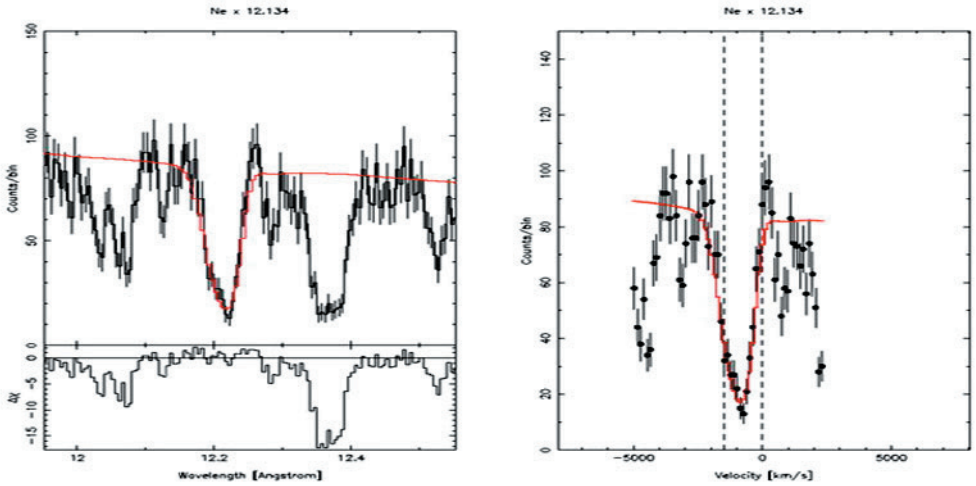

FIGURE 17: Histogram data of Ne X and neighboring absorption lines with model and continuum overplotted, shown in both wavelength (left) and velocity (right) space. (From Ramirez et al., Fig.3)

Of course, NGC 3783 is not the only Seyfert AGN to be observed with the HETGS; it is just one of many "good reads" available in the *Chandra* archive. To make these data more available to the general astronomy community, a *Chandra* archival grant was awarded to make a database of HETGS AGN products that are in "ready to go" format, e.g., rest-frame fluxed spectra. Although in development now, keep your eye on the "Hot Gas" web page [10] and/or send a request to the e-mail address on that web page to be informed when it is online. And... enjoy the stories!

Dan Dewey, for the HETG team.

References

[0] *Chandra* 2005 Cal Workshop: http://cxc.harvard.edu/ccw/proceedings/05_proc/index.html

[1] HETG calibration: http://space.mit.edu/CXC/calib/

[2] Canizares et al, 2005, PASP 117, 1144.

[3] Kaspi et al. 2001, ApJ, 554, 216.

[4] Kaspi et al. 2002, ApJ, 574, 643.

[5] Holczer, T., Behar, E., and Kaspi, S. 2005, ApJ, 632, 788.

[6] Chelouche, D. and Netzer, H. 2005, ApJ, 625, 95.

[7] Ramirez, J.M., Bautista, M. and Kallman, T. 2005, ApJ, 627, 166.

[8] Krongold, Y., Nicastro, F., Brickhouse, N.S., Elvis, M., and Mathur, S. 2005, ApJ, 622, 842.

[9] Yaqoob, T., Reeves, J.N., Markowitz, A., Serlemitos, P.J., and Padmanabhan, U. 2005, 627, 156.

[10] Hot Gas web page: http://hotgas.pha.jhu.edu

Instruments: LETG

LETG Calibration: Variable Standards

Excuse my scribbling, it is late, and I have a poor candle.
-Henri Rousseau

Painting the jungles of the imagination seems a wise choice compared with navigating the jungles of X-ray calibration. Excuse my cringeworthy metaphors, this article is late, and I have a poor set of standard candles.

The irony of the term ``standard candle'' is actually quite appropriate here---what candle could ever be a standard? In an uncontrolled environment, like my office, which appears to be entirely out of my control, a candle flame flickers[1] like any good cosmic point source of X-rays. The British Parliamentary Standard Candle of 1860 called for spermaceti with a melting point of 112-115° F mixed with a small amount of beeswax. The length was 10 inches, the bottom diameter 0.9 inches and the top diameter 0.8 inches. Even under controlled conditions its burn rate varied by 5% - still a good enough number for most X-ray calibration work though. Using paraffin wax and controlling the precise chemical composition of the candle helps with luminous stability (and keeps the sperm whales happy), as does a more precise specification of diameter and wick. Using the standard lamps and candles to light big fat cigars and adopting a simple definition of luminance based on the power of the source is even better, which is more or less what those *Systéme International* folk did in 1979.

Hot white dwarfs make the best point source standard candles in the EUV and very soft X-rays. The LETGS uses two of them, Sirius~B and HZ~43, as effective area calibrators in the 60 - 170 Å range. The HRC-S detector used with the LETG was not absolutely calibrated on the ground below the energy of the C inner shell Kα line at 277 eV (44.76 Å). However, the LETG+HRC-S effective area can be derived simply by dividing the observed raw spectrum of a standard candle by its model spectrum. Model spectra are computed for the appropriate stellar parameters using the fully non-LTE radiative and hydrostatic equilibrium model atmosphere programs PRO2 (developed by Klaus Werner and co-workers, University of Tübingen) and TLUSTY (developed by Ivan Hubeny and Thierry Lanz, NASA GSFC). We can obtain sufficient signal for a quite precise calibration (to a few percent on a ~ 1Å scale) in about 50ks of exposure time: the problem is not precision but accuracy - like the difference between "precision cosmology'' and "accurate cosmology''. While the stars

[1]Fortunately, a nearby fire extinguisher saved a nova-like conflagration and I managed to save one of my two colouring books.

themselves are, for our purposes at least, constant, unwavering X-ray beacons of hope, the models of their emission are not. These models flicker in the winds of model atmosphere change. In the last several years, both atmosphere modelling groups have reported improvements, such as in the treatment of Lyman and Balmer line blanketing, and in Gaunt factors. These lead to palpable changes in predicted soft X-ray spectra.

Fanned by a strengthening gale of model atmosphere change, our standard candles seemed to be going Roman at the *6 Years of Science with Chandra Symposium* at the beginning of November last year (appropriately close to Guy Fawkes Night[2]). Electron scattering is an important opacity source in hot DA white dwarf atmospheres. Models currently employ Thomson isotropic scattering, whereby only the direction of photon propagation changes as the result of a scattering event. More rigorously, finite electron mass instead implies that both momentum and energy exchange should actually occur. Photon energies are reduced by each scattering event, such that emergent spectra are expected to be softer in X-rays when Compton Scattering is accounted for (though it is not quite so simple since Compton Scattering also induces a change in atmospheric temperature structure). Estimates made by Jerzy Madej (1998) for HZ43 suggested the frequency redistribution effects would only become significant at wavelengths < 50Å, where the flux is too low to be of any use for calibrating *Chandra*. At the Calibration Workshop, Jelle Kaastra (SRON) and co-workers suggested, based on new calculations, that Compton Scattering might be important after all, causing differences at wavelengths > 50 Å of more than 20% in emergent soft X-ray flux for both Sirius B and HZ43 compared with models using Thomson scattering. Jerzy Madej (University of Warsaw Astronomical Observatory) and Valery Suleimanov (Tübingen University) managed to dowse the flames by re-examining the problem with their customary rigour: new calculations, designed to avoid numerical pitfalls of earlier methods, show Compton scattering to be completely negligible for wavelengths longer than ~25 Å or so, where the flux is so weak and dependent on the exact temperature structure of the atmosphere model that other uncertainties dominate predictions by orders of magnitude. So, I think we can draw a line under that one. Now, if only people would let sleeping dog stars lie.

You cannot be Sirius (B)

At the time of the launch of *Chandra*, both Sirius B and HZ 43 appeared to have fairly well-defined physical parameters based on optical, UV and EUV observations. The most important for understanding the soft X-ray flux is effective temperature, though surface gravity (controlling the atmospheric gas pressure) also interferes in the process. In the case of Sirius B, many years of astrometric measurements of the binary enable a reasonably accurate mass estimate. The precise (and hopefully accurate) parallax enables comparison of spectroscopic and astrometric mass estimates and accordance inspires a greater degree of confidence in the fidelity of the absolute flux of model atmosphere predictions outside of the ranges amenable to accurate absolute flux measurement - soft X-rays perhaps.

The effective temperature and surface gravity of a DA white dwarf can be determined from the Balmer series. Until recently, the glare from Sirius A has prevented acquisition of a high quality uncontaminated visible light spectrum of Sirius B. However, since 1993 the trajectories of Sirius A and B have been taking them farther apart on the sky and Barstow et al. (2005) were recently able to obtain an HST STIS spectrum of Sirius B. From this they estimated a temperature T_{eff}= 25,193 ± 37 K and gravity log g = 8.556 ± 0.010 - extremely precise measurements, though the formal uncertainties do not account for modelling systematics and uncertainties in underlying input data and physics in the atmospheric and radiative transfer modelling. The formal uncertainties also do not encompass the earlier temperature estimate of 24790 ± 100 K derived by Holberg et al. (1998) from *IUE* and *EUVE* observations (the surface gravity instead agrees with the older estimate of log g = 8.57 ± 0.06). The 1.5% difference between new and older temperatures seems a bit picky - it does not change the UV-optical spectrum appreciably - but unfortunately we are interested in the Wien tail which is exponentially sensitive to temperature.

Collaborations with Martin Barstow (University of Leicester) and Klaus Werner and Thomas Rauch (Tübingen University) aimed at a better understanding of the X-ray spectral energy distributions of HZ43 and Sirius B are ongoing. Catastrophic implications for the low energy LETG+HRC-S calibration are avoided by the necessity of matching existing *EUVE* data in the 100 Å range. *EUVE* detectors were calibrated on the ground to an absolute accuracy of 20% or so, so any changes to the lowest energy calibration of *Chandra* should be no larger than this. The existing stated uncertainty of the LETG+HRC-S effective area in the 60-170 Å range is 15%. A revision of this magnitude over the next 12 months is quite possible.

LETG Science: LETG Observes Purple Haze

AGN are versatile fellows: disks, winds, jets, putative black holes, absorption lines, emission lines; they have it all. A couple of years back, Pounds et al. (2003) observed the narrow emission line quasar PG1211+143 with *XMM-Newton* and found blueshifts of 24000 km s^{-1} in the absorption lines of H- and He-like ions of Fe, S, Mg, Ne, O, N and C. Pounds et al. interpreted the absorption as arising in a massive outflow---with a mass and kinetic energy comparable to the accretion mass and total luminosity of the source.

PG 1211+143 was observed again in June 2004, this time using the *Chandra* LETG+ACIS. From this observation, Reeves et al. (2005) detected absorption lines at 4.22 and 4.93 keV, corresponding to 4.56 and 5.33 keV in the rest frame of

[2]November 5. Guy Fawkes---from whom the word ``guy'' derives---was hung, drawn and quartered for his part in the Gunpowder Plot to kill King James and the ruling aristocracy by blowing up the Houses of Parliament during its state opening in 1605

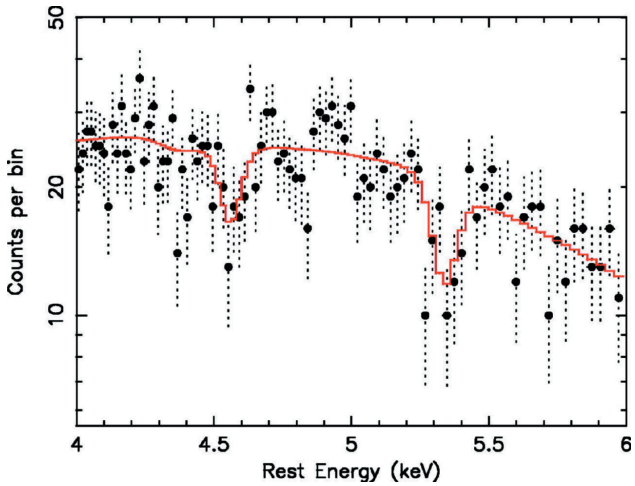

FIGURE 18: LETG+ACIS-S spectrum of PG 1211+143, transformed to the rest frame, in the 4 - 6 keV range, binned at 0.0125 Å intervals. Data (filled circles), 1σ error bars (dotted lines) and the best-fit absorption-line model are shown. If identified with Fe XXVI Lyα, the redshift of each line would correspond to velocities of 0.26c and 0.40c. Such redshifts could result from matter from a massive outflow falling back onto the central black hole. From Reeves et al. (2005).

PG 1211+143. Since there are no obvious transitions at these energies that would be expected to give rise to such absorption, either in the rest frame or at 24000 km s^{-1}, Reeves et al. concluded that the most likely culprit is highly redshifted ionized Fe XXV or Fe XXVI. The relativistic velocity shifts required for such redshifts are rather large - 0.40c and 0.26c. To explain such redshifts by gravity alone would require matter in a stable orbit within 6 gravitational radii of the black hole. As Reeves et al. note, this is within the last stable orbit around a Schwarzschild black hole and would require a Kerr metric. Alternatively, Reeves et al. suggest the data could also be explained by matter falling directly onto a central black hole. One possible origin for such matter might be fall-back from part of the massive 24000 km s^{-1} outflow found from the *XMM-Newton* observation that does not escape the central gravitational potential. Redshifts and blueshifts at the same time. Or, as concisely summarised by Jimi Hendrix, *"Purple haze all around, Don't know if I'm comin' up or down"*.

Observer and proposer information and news on the performance of the *Chandra* LETGS can be found on the instruments and calibration page: http://cxc.harvard.edu/cal/Links/Letg/User/

Jeremy Drake for the LETG team

Barstow, M. A., Bond, H. E., Holberg, J. B., Burleigh, M. R., Hubeny, I., & Koester, D. 2005, MNRAS, 362, 1134
Holberg, J. B., Barstow, M. A., Bruhweiler, F. C., Cruise, A. M., & Penny, A. J. 1998, ApJ, 497, 935
Madej, J. 1998, A&Ap, 340, 617
Pounds, K. A., Reeves, J. N., King, A. R., Page, K. L., O'Brien, P. T., & Turner, M. J. L. 2003, MNRAS, 345, 705
Reeves, J. N., Pounds, K., Uttley, P., Kraemer, S., Mushotzky, R., Yaqoob, T., George, I. M., & Turner, T. J. 2005, ApJL, 633, L81

Pitch Angle Restrictions

As thermal conditions on the spacecraft have changed, some new limitations on observations have been added. In order to avoid overheating the charged particle detector, EPHIN, or excessive cooling of the propellant lines, the maximum length of an exposure is dependent on the pitch angle of the target.

As a reminder of the new situation, we have excerpted parts of section 3.3.2 of the AO 8 POG. *(Editor)*

*** ***Proposers and observers, however, should check the CXC website for any changes in the restrictions***. ****

Constraints necessary to ensure the health and safety of the spacecraft and science instruments.

Sun avoidance: (cannot be overridden) Restricts viewing to angles larger than 46° from the limb of the Sun. This restriction makes about 15% of the sky inaccessible on any given date, but no part of the sky is ever inaccessible for more than 3 months.

Pitch angle constraints: Changes in the thermal properties of the spacecraft with time are introducing additional restrictions in the solar pitch angles (i.e., angles between the viewing direction and the direction to the sun, see Figure 19) that can be observed. These restrictions are evolving with time; **observers are urged to consult the CXC web pages for the latest developments**. The pitch restrictions are of two kinds:

a. The EPHIN detector is subject to possibly degraded perfor-

Angle Range	Restriction	Reason
0 - 45	No observations	HRMA Sun avoidance
45 - 65	Unrestricted	
65 - 135	~50 - 100 ks orbit, depending on pitch history	EPHIN temperature limitations
135 - 152	Unrestricted	
152 - 170	7 to 40 ks observation, depending on length of previous attitude at low pitch angle	Propulsion line temperature
170 - 180	No observations	Propulsion line temperature limitations

TABLE 1: *Chandra* observing limitations due to solar pitch angle constraints. Get the most recent numbers from the CXC web pages.

mance at elevated temperatures that may affect its use in safing the science instruments from high levels of particle radiation. During long observations at pitch angles of between approximately 65 and 135 degrees the EPHIN may reach temperatures that may result in anomalous performance depending on its prior thermal history. A model of the EPHIN temperature as a function of pitch profile has been developed that is used in planning to constrain the maximum EPHIN temperature.

b. Due to occurrences of excessive cooling in propellant lines, we are implementing a restriction against pointing at pitch angles greater than 170 degrees. For Cycle 8 we urge that you carefully consider how to configure your observation such that it does not require a pitch angle greater than 170 degrees. This may be done, for example, by imposing no constraints on the observation, or by checking that the time or roll constraints can be satisfied with the target at angles between 45 and 170 degrees from the sun (subject to the EPHIN-related pitch constraints described above). Even if accepted by the peer review, it may subsequently turn out that observations which can only be accommodated at pitch angles greater than 170 degrees simply will not be done. Further, there are observing restrictions in the pitch angle range 152-170 degrees imposed by the need to prevent propellant lines from dipping to excessively low temperatures before line heaters switch on.

These spacecraft constraints have several implications for proposers:

• Observations in the adverse 65-135 degree pitch zone can be done, but if long will be broken into shorter durations, which may be separated by a day or more. The maximum continuous duration may be in the vicinity of 30 ks, but is dependent on the preceding pitch angle history of the observatory. If such observations have roll constraints, the observations must either be brief or the roll constraints must be generous enough to allow multiple segments at their different, time-dependent roll angles. Constraining roll angles to be constant for multiple segments

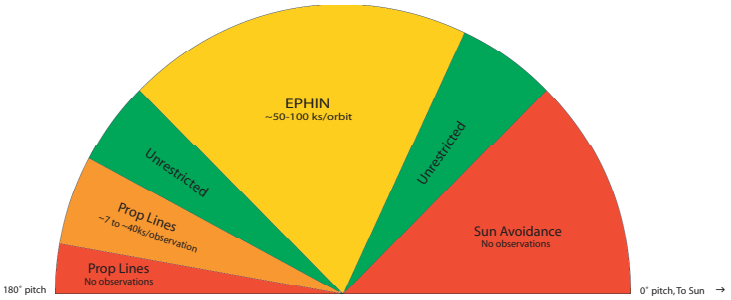

FIGURE 19: Diagram to illustrate ranges of solar pitch angle (the angle between the pointing direction and the satellite-Sun line) within which different observing limitations apply. Table 1 provides quantitative estimates for the observing limitations in the solar pitch angle ranges shown in the drawing.

is discouraged, as achieving off-nominal roll angles may present thermal difficulties.

• Observations at pitch angles outside but near near the 65-135 degree zone may also be segmented if the EPHIN thermal prediction model shows a possibility of overheating.

• Simultaneous longer-duration observations with telescopes (such as XMM-Newton) with a preferred pitch angle in the 65-135 degree range may be very difficult, or even impossible, to schedule.

• Targets near the ecliptic poles (such as the Magellanic Clouds) are especially affected since their pitch angles are always close to 90 degrees.

Finally, proposers should check that time (or equivalently roll) constrained observations do not force *Chandra* to unfavorable pitch angles unless the observations are short or can be segmented. Visibility, roll, and pitch for any sky position as a function of time can be viewed using the ObsVis, either through the web interface or for download, under Observation Visualization and Planning at http://obsvis.harvard.edu/.

Adapted from the *Chandra* Proposers' Observatory Guide (POG), Rev. 8.0, Dec. 2005

Useful Chandra Web Addresses

To Change Your Mailing Address:	http://cxc.harvard.edu/cdo/udb/userdat.html
CXC:	http://chandra.harvard.edu/
CXC Science Support:	http://cxc.harvard.edu/
CXC Education and Outreach:	http://chandra.harvard.edu/pub.html
ACIS: Penn State:	http://www.astro.psu.edu/xray/axaf/
High Resolution Camera:	http://hea-www.harvard.edu/HRC/HomePage.html
HETG: MIT:	http://space.mit.edu/HETG/
LETG: MPE:	http://wave.xray.mpe.mpg.de/axaf/
LETG: SRON:	http://www.sron.nl/divisions/hea/chandra/
CIAO:	http://cxc.harvard.edu/ciao/
MARX simulator:	http://space.mit.edu/ASC/MARX/
MSFC: Project Science:	http://wwwastro.msfc.nasa.gov/xray/axafps.html

Chandra/HST/Radio Observations of NGC 2110

NGC 2110 has historically been classified as a narrow emission-line galaxy, which is the subclass of Seyfert galaxies with strong 2-10 keV X-ray emission and narrow (< 600 km/s) optical emission lines. Observations with the VLA (e.g., Ulvestad & Wilson 1989) show it is the parent galaxy of an S-shaped jet-counterjet system that extends 4" in the N-S direction. Optical emission-line studies (e.g. Mulchaey et al. 1994; Ferruit et al. 2004) reveal a similar-shaped distribution of [O III] which, interestingly, is not spatially coincident with the radio emission. ROSAT observations (Weaver et al. 1995) first hinted at the presence of extended circumnuclear X-ray emission in NGC 2110, the spatial and spectral details of which we can now investigate in detail by taking advantage of the superb angular and spectral resolution of *Chandra*.

Figure 21 shows a smoothed tri-band *Chandra* ACIS-S image of NGC 2110 combined over 3 different observing modes (ACIS-S in VF mode, ACIS-S + HETGS in alternating frame mode, ACIS-S+HETGS in TE mode) in 3 AOs. The extended emission is dominated by soft X-ray photons, in contrast to the nuclear emission, where a significant fraction of the hard (> ~3 keV) X-rays are concentrated. This is consistent with our preliminary findings from the combined ~210 ks HETGS spectrum , which shows a strong Fe Kα emission line that may have origins in both the torus and accretion disk (Figure 20).

A multi-wavelength overlay of the emitting regions (Figure 22) shows the X-ray emission to be offset from the radio (5-GHz VLA), but coincident with the HST [O III]. While it is known that the radio is associated with a small-scale jet, we speculate that X-ray and [O III] may have common origins in the form of reprocessed nuclear radiation, or more exotically, in gas shock-heated by the radio jet.

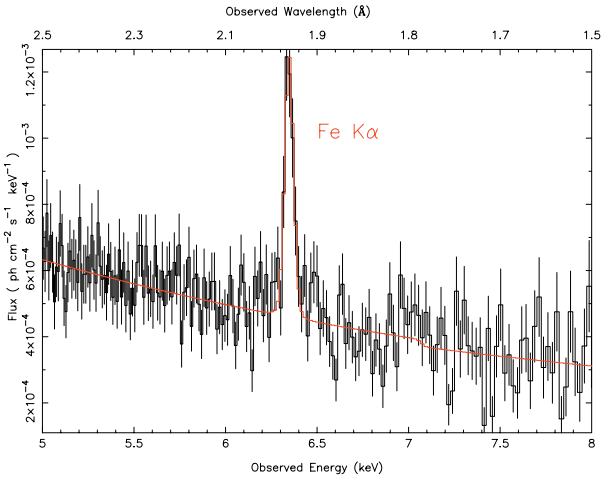

FIGURE 20: *Chandra* HEG spectrum of NGC 2110 binned to 0.01Å. Over-plotted (red) is the convolved best fit model for continuum and Fe Kα emission line.

Dan Evans, Julia Lee (Harvard), Sarah Gallagher (UCLA)

References

Ferruit, P., et al., 2004, MNRAS, 352, 1180
Mulchaey, J. S., et al., 1994, ApJ, 433, 625
Ulvestad, J. S., Wilson, A. S., 1989, ApJ, 343, 659
Weaver, K. A., et al., 1995, ApJ, 442, 597

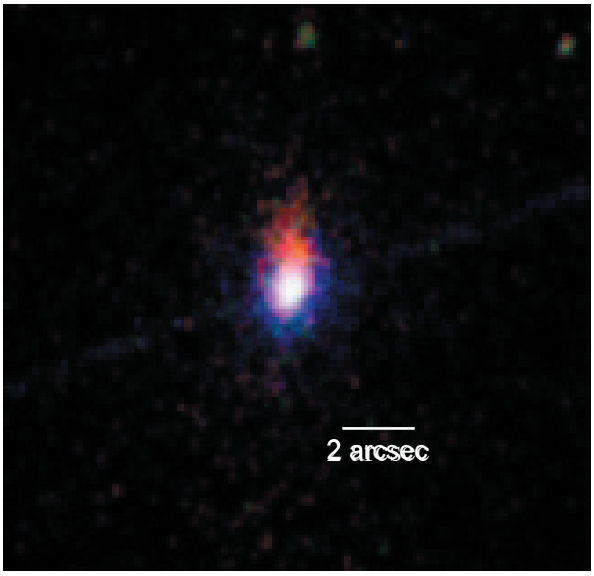

FIGURE 21:Tri-color (red: 0.5-1 keV, green: 1-1.5 keV, blue: 4-5 keV) ACIS-S image of NGC 2110 shows extended emission prevalent towards the north.

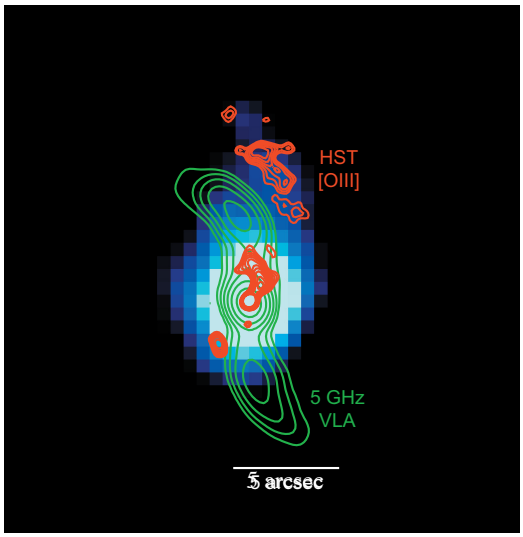

FIGURE 22: The 0.5-1.5 keV ACIS image of NGC 2110 (blue) with VLA (green) and HST [OIII] (red) contours overlaid.

CXC 2005 Science Press Releases

See http://chandra.harvard.edu/press/press_release.html for more details.

Table 2 - *Chandra* 2005 press releases.

Date	PI	Objects	Title
28 Dec 05	Elsner	Earth	Chandra Looks Back at the Earth
1 Dec 05	Fabian	Perseus Cluster	Chandra Proves Black Hole Influence is Far-Reaching
29 Nov 05	Immler	SN 1970G	NASA Scientists Witness Cosmic Rite of Passage
2 Nov 05	Muno	Westerlund 1	Neutron Star Discovered Where Black Hole Was Expected
13 Oct 05	Nayakshin	SGR A*	Stars Form Surprisingly Close to Milky Way's Black Hole
5 Oct 05	Fox	GRB 050709	In a Flash, NASA Helps Solve 35-Year-Old Mystery
22 Sep 05	Hughes	Tycho	Tycho's Remnant Provides Shocking Evidence for Cosmic Rays
7 July 05	Drake	21 nearby, Sunlike stars	NASA's Chandra Neon Discovery Solves Solar Paradox
30 May 05	Strohmayer	RX J0806.3+1527	NASA Sees Orbiting Stars Flooding Space with Gravitational Waves
25 May 05	Bhardwaj	Saturn	NASA's Chandra Finds that Saturn Reflects X-rays from Sun
10 May 05	Feigelson	Orion	Planetary Protection: X-ray Super-Flares Aid Formation of "Solar Systems"
28 Apr 05	Karovska	Mira	"Wonderful" Star Reveals its Hot Nature
19 Apr 05	Safi-Harb	G21.5-0.9	Cosmic Shell-Seekers Find a Beauty
6 Apr 05	Alexander	Sub-mm galaxies in CDF-N	Era of Galaxy and Black Hole Growth Spurt Discovered
22 Mar 05	Liu	M74	X-rays Signal Presence of Elusive Intermediate-Mass Black Hole
2 Mar 05	Elsner	Jupiter	Chandra Probes High-Voltage Auroras on Jupiter
15 Feb 05	Barger	Lockman Hole	NASA Observatory Confirms Black Hole Limits
2 Feb 05	Nicastro	Mkn 421	Lost and Found: X-ray Telescope Locates Missing Matter
10 Jan 05	Muno	Galactic Center X-ray Binaries	Chandra Finds Evidence for Swarm of Black Holes Near the Galactic Center
5 Jan 05	McNamara	MS 0735.6_7421	Most Powerful Eruption in the Universe Discovered

Megan Watzke

Testing of CIAO

Reprinted by permission from *ADASS XV Proceedings* (Escorial, Spain, 2005) ASP Conf. Ser., G. Gabriel, C. Arviset, D. Ponz, and E. Solano, eds.

Introduction

Chandra Interactive Analysis of Observations (CIAO) consists of a suite of tools and applications developed for the analysis of *Chandra X-ray Observatory* data. With its unprecedented technical capabilities and science potential, *Chandra* requires a novel, flexible, multi-dimensional set of tools for data analysis. This mission provides 4-dimensional data (2 spatial-dimensions, time, & energy), each containing many independent elements. *CIAO* tools are able to filter and project the 4-dimensional event data to manageable sizes and convenient arrays in an easy and flexible manner. *CIAO* is a mission independent system and can be used for data analysis of other X-ray and non- X-ray observations.

Since launch there have been several major *CIAO* releases. A major step in the preparation of each *CIAO* release is scientific and functional testing of the software. This is a joint effort by the *Chandra X-ray Center Data Systems (DS)* and *Science Data Systems (SDS)* teams. We highlight here the stages of *CIAO* testing and the procedures we follow at each stage.

CIAO Tool Development

The *CIAO* tool development process begins many months before a planned release. SDS scientists identify and evaluate science and calibration milestones for *Chandra* data analysis, and outline the priorities and goals for tool and application development for a *CIAO* release.

During the software development process scientists and developers interact closely to assure *CIAO* tools are designed and built to the specified requirements and that they follow *CIAO* system standards.

Once implemented, unit tests are developed and run to assure proper implementation. We recognize that more rigid tests are required though, and science and development teams combine efforts to ensure this goal is met.

CIAO Release Testing

CIAO releases involve 4 testing stages. These are: (1) unit testing, where detailed tests of *CIAO* tools verify and validate the correct implementation of scientific algorithms; (2) mini-testing, where the new functionality of the system is bundled and tested across ported platforms; (3) regression testing, where baseline system tests are run on all ported platforms to validate the system; and (4) package testing, where tar files are downloaded from the public web page to validate web links, instructions, and the software installation.

Science Unit Testing

Unit science tests are developed for each new or updated tool as they are completed by the software team. It is in this testing phase that scientists run tools they have specified for the first time. Unit tool testers verify and validate that the tool was implemented as they envisioned with correct and robust algorithms to meet the science goals. They also run the tools in science data analysis scenarios where the output file of one tool is provided as the input to the next in a series of tool steps organized to meet specific science goals. It is these science scenarios that really separate science testing from the software team testing.

A tool that is run standalone (as in development unit test) is less rigorously tested than one that is run as part of a data analysis thread where tool's functionality is judged, not only the tool execution and creation of output data, but whether the data product provides all of the input required to do further analysis with other tools. The output products of one tool are often the input to many tools that utilize those data to do further analysis. It is sometimes found that there are keywords missing in a file header, or table columns written by a tool have missing information or are problematic with other programs that read those data products. Sometimes the software upgrades are in software libraries. In those cases we identify tools that explicitly utilize the enhancement or bug fix for this level of testing.

A science tester first outlines a plan based on the requirements for the tool, their expectations of the tools flexibility, and the range of parameters and data the tool was specified to work with. They have often already provided baseline datasets and use-cases for the developers unit test. At this stage the goal is to catch missing details in the specification or implementation of the tool.

Once there is a plan, the scientist runs the commands or builds a script to test the tool. Often iteration with the development team starts at this point. E-mails are sent to an internal alias where they are being stored; They are accessible from an e-mail archive. During this process questions are asked, issues are uncovered, and interpretation of requirements is discussed. Developers address reported problems and make bug fixes and enhancements to the tool. E-mail messages also seed bug reports that track problems.

The unit testing stage is completed either with successful completion of the unit test, or by identifying that the uncovered problem would require a longer time-frame for solving. Each unit tester captures the testing steps along with the input and output data, and prepares a unit test worksheet.

The test worksheet is a means to communicate the status of unit testing, and when success is indicated, it is the trigger to have the test added to the regression suite. Tests are run across all platforms of a *CIAO* release to verify that there are no porting issues.

Each test worksheet contains information on the tool status, level of completion of unit testing, and a log of the test session and/or a pointer to a test script. Furthermore, it contains pointers to input data, and to datasets created as output from the tool. The test worksheets are then used as input to build automated regression test scripts. Scientists work to validate the tool on their computer platform of choice. The work to validate the tools across ported platforms is for most part performed automatically.

When unit testing is completed, and the issues related to a given tool are resolved, the tool lead indicates that testing was successful and the tool is ready for release. Sometimes it is at this point that a tool is rejected from the upcoming release, or if the tool is required for a successful release, the schedule is extended to allow time to address the problem that must be solved.

Mini-testing

Over the few weeks of testing following a code freeze, the *CIAO* system is built bi-weekly to bring tools that have had problems addressed back to the release configuration. They are re-tested by unit testers until they are ready to complete a new test worksheet. At this time, a targeted regression test is built that contains a sample of previously released *CIAO* tools, the new or modified tools, and tools that exploit the functions added to libraries. This test set is small so it runs quickly and is aimed at exercising the highest risk areas of the software. Since the test script consists of a subset of what would become the full regression test, we refer to this as the mini-test. The mini-test is run once the first build of the system is completed after a code freeze, and almost weekly during the period of rebuild and science unit testing to ensure software stability over all platforms.

Later in the release cycle, the software tests outlined in the test worksheets are added to the regression test script. The output results of the current execution are compared to data saved from previous runs. Some of these data are from the last *CIAO* release, while new tests use data provided with the test worksheet. When the mini-test is upgraded with the worksheet tests, we refer to it as the mini+ test.

Full regression testing

Late in the release schedule, a full regression test is run and results are verified on all platforms. This test is the culmination of all test scripts written since the start of *CIAO* development. New tests outlined in the test worksheets are added for each release. This test is usually run once, late in the release cycle, across all ported platforms, and the results verified against previous runs of the tools.

An important part of this step is the overall test evaluation by the SDS testing lead. The unit tests, mini tests, and full regression tests are reviewed and evaluated, and upon successful completion, the test lead signs off that science testing is complete and the tools are ready for release. With sign-off of science testing, we move into download testing which is the last step in the release testing process.

Download testing

In download testing, the system as packaged for release is posted to a hidden public web page. Scientists assigned to verify downloads on various platforms supported by *CIAO*, practice a download and installation of the system. Installation instructions are reviewed, web links and tar files validated, and the system is spot checked. The development team provides a download test script which runs a sample set of *CIAO* tools. The script reports whether the test is successful. At this stage we evaluate success based on the execution of a tool and not a comparison to previous results.

Both science and development leads evaluate the readiness for release, and upon successful completion of download testing give their concurrence to make the system available for public download.

Summary

The test procedures described here, have been developed over the 6 years of the *Chandra* mission. This framework has assisted us in making 3 major releases and 6 minor releases of *CIAO*. We generally support ports to Sun, several flavors of Linux, and Mac systems. *CIAO* consists of approximately 80 command line tools and several large applications. Our release schedule is well defined.

Our process is sometimes adapted to specific circumstances but well within the framework described here. We have found these steps very helpful to achieve stable and successful *CIAO* releases.

M. Karovska, J. D. Evans, and the CIAO testing team

Acknowledgements

The testing of *CIAO* is carried out by members of *Chandra X-ray Center Science Data Systems* and *Data Systems* teams. Support for this work is provided by the *National Aeronautics and Space Administration* through the *Chandra X-ray Center*, which is operated by the *Smithsonian Astrophysical Observatory* for and on behalf of the *National Aeronautics and Space Administration* under contract NAS 8-03060.

Detailed information on *Chandra X-ray Observatory* and *CIAO* can be found in: http://cxc.harvard.edu/ciao/

Validation and Verification of Chandra Data: A New and Improved system

(Adapted from ADASS05 paper titled "Validation and Verification: Combining pipelines, a Graphical Application and the Human Factor" by Janet DePonte Evans, Thomas J. Calderwood, Ian N. Evans, Kenny J. Glotfelty, Diane M. Hall, Joseph B. Miller, and David A. Plummer)

contact: janet@cfa.harvard.edu

Introduction

Over the past year, *Chandra* observers will have noticed a new Verification and Validation (V&V) report added to the data products available from Standard Data Processing (SDP). The report is just the end product of a new and improved V&V system developed by the *Chandra* Data System based on mission experience and characterization of known issues by instrument scientists.

V&V is performed on each observation processed through the SDP pipelines. A V&V pipeline runs at the end of observation processing (L2). A manager component is then triggered and controls the V&V flow after the pipeline completes. A GUI provides the user interface to the operations staff for data quality review.

Validation and Verification Requirements

The V&V system provides 2 distinct checks for data quality assurance: validation and verification.

Validation applies a set of predefined tests to the SDP data products to ensure processing and calibration were performed correctly. Some validation requirements are easy to predefine (for example, searching pipeline processing logs for errors). Others require mission experience to understand the boundary between processing, calibration and performance limitations and actual anomalous behavior. If an observation fails validation, the SDP operations staff must be notified that reprocessing of the observation is required.

Verification compares the actual spacecraft and instrument configurations with the requested configurations, and checks that the scheduling properties of the observation meet the constraints specified by the observer. If an observation fails verification, the *Chandra* Director's Office (CDO) must be notified, along with the relevant instrument scientist (if appropriate).

Secondary requirements of V&V include: (1) creating a written report that is accessible to the observer; (2) updating an observation's *charge time* in the *Observation Catalog* database, which is counted against the target's time allocation to determine if additional scheduling is required to complete the observation; (3) triggering promotion of data products in the *Chandra Data Archive* to identify the data products as the default versions available to users; (4) triggering data distribution (or feedback for reprocessing); (5)~initiating the start of the proprietary period clock (for observations with proprietary data rights); and (6) enabling the reviewer to complete V&V in ~5 minutes for a successfully processed observation.

Automated Validation and Verification Design

The design goals of our post-launch efforts were aimed at encapsulating experience gathered with the live mission into automated checking. This included limit-checking only *pertinent* science and engineering data, identifying *specific* serious pipeline warnings and errors, and presenting and evaluating carefully *selected* data views defined by V&V and instrument scientists based on experience. Human review is minimized by identifying unexpected test results using color coding.

To improve system integrity and automation goals, the V&V software also manages all of the required interfaces and system triggers, including triggering an error recovery path - reprocessing, rescheduling, and further investigation by instrument teams. Other design goals included enabling other groups to evaluate V&V by providing an interface to CDO and instrument scientists, and allowing off-site access via a standard web browser to support rapid turnaround of fast processing requests or anomaly resolution.

Automated Validation and Verification Implementation

The V&V software is implemented as three components: (1) a pipeline, which executes after the completion of level 2 processing for an observation; (2) a manager process that controls the V&V flow after the pipeline completes; and (3) a GUI that provides the user interface for the reviewer.

The pipeline creates the V&V data products that are displayed through the GUI, including predefined html web-pages, JPEG images, PNG plots, and key tabular information designed specifically for V&V. The pipeline also creates a template PDF format report for distribution to the user, and seeds the report with textu-

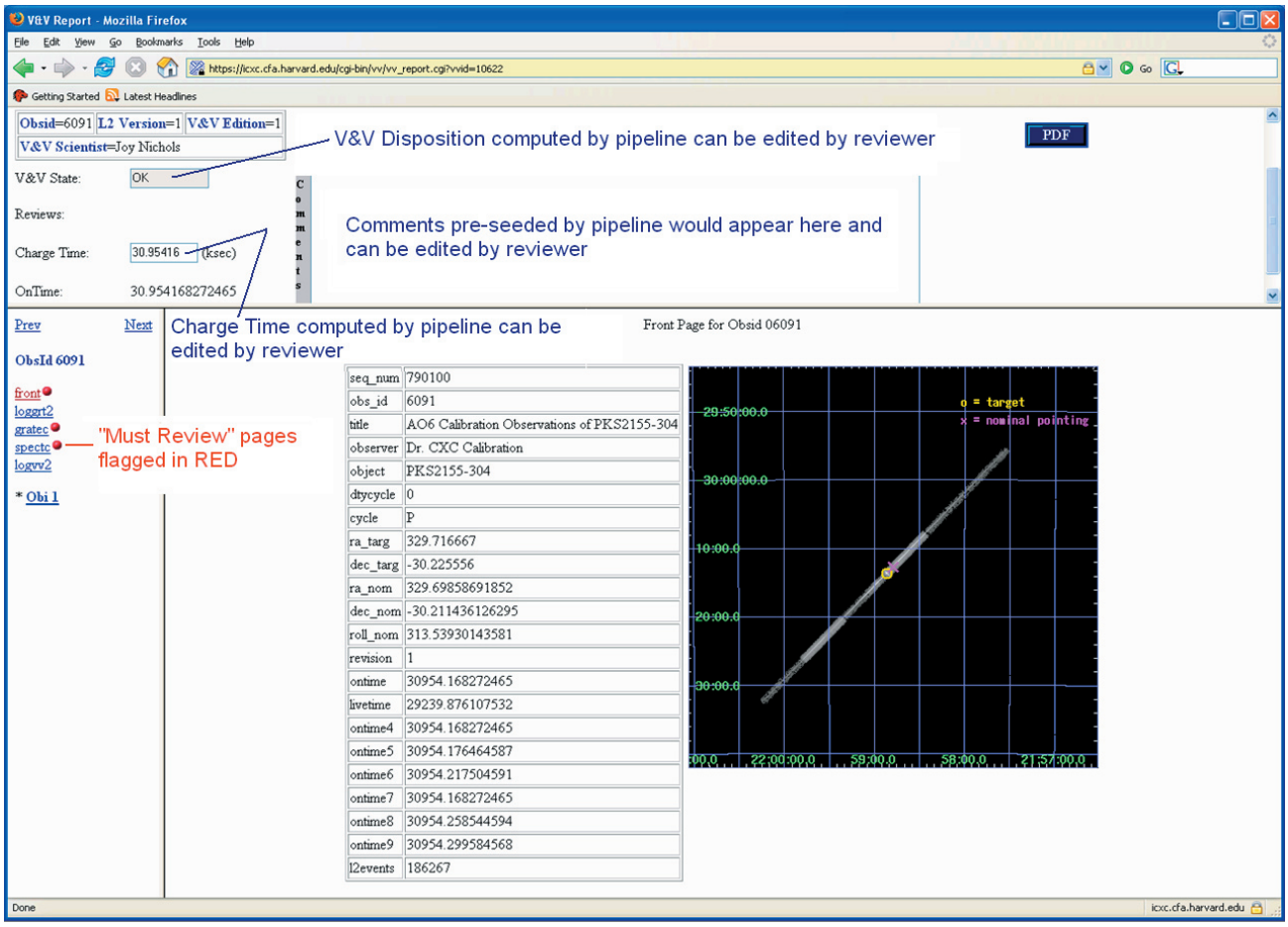

FIGURE 23: Sample V&V GUI observation front page.

al comments and the "most likely" disposition status based on the results of the tests applied by the pipeline. Finally, the pipeline computes the nominal charge time for the observation.

The manager builds and links the V&V report web-pages into the GUI for display to the reviewer, and manages any input that the reviewer may supply using the GUI, including verifying that any revisions to the calculated charge time comply with appropriate rules. State transition updates occur when a new disposition status is selected by a reviewer for an observation, and initiate further actions by the manager process, such as sending email notifications to appropriate parties, or triggering data distribution. The manager also creates the final V&V report for distribution to the user by incorporating the reviewer comments and disposition status entered via the GUI into the template report. This last action is triggered when the reviewer submits a final state as the disposition status for the observation, indicating that the review is complete.

The GUI is the interface for the reviewers and others handling V&V. It guides the reviewers through the evaluation process by identifying required ("must review") and supporting data views, and provides the capabilities to edit the comments, charge time, and disposition status seeded by the pipeline. The GUI also provides mechanisms to manage authorized users of the V&V software, including their privileges (which define the functions that they may perform) and their capabilities (which identify the types of data that they may handle). The GUI provides a selectable set of mechanisms to assign reviews to reviewers based on comparison of the actual instrument configuration and scientist's capabilities. Finally, the GUI triggers creation of a new edition of a report if it must be revised after submission with a final state.

The new V&V software was installed in operations in January 2005. It provides a systematic evaluation of SDP results and issues, and allows operations staff to perform V&V. As a result, the data processing statistics have improved dramatically and the quality of the data products to the user has improved.

Janet DePonte Evans

Chandra Users' Committee Membership List

The Users' Committee represents the larger astronomical community. If you have concerns about *Chandra*, contact one of the members listed below.

Name	Organization	Email
Vassiliki Kalogera	Northwestern	vicky@northwestern.edu
Julia Lee	Harvard	jclee@cfa.harvard.edu
Knox Long	STScI	long@stsci.edu
Smita Mathur	OSU	smita@astronomy.ohio-state.edu
Chris Mauche	LLNL	mauche@cygnus.llnl.gov
Kazuhisa Mitsuda	ISAS, Japan	mitsuda@astro.isas.ac.jp
Chris Reynolds (Chair)	University of Maryland	chris@astro.umd.edu
Maria Santos-Lleo	XMM	msantos@xmm.vilspa.esa.es
Steve Snowden	GSFC	snowden@riva.gsfc.nasa.gov
Lisa Storrie-Lombardi	Spitzer Science Center	lisa@ipac.caltech.edu
Leisa Townsley	PSU	townsley@astro.psu.edu

Ex Officio, Non-Voting

Alan Smale	NASA HQ	Alan.P.Smale@hq.nasa.gov
Wilt Sanders	NASA HQ	wsanders@hq.nasa.gov
Allyn Tennant	NASA/MSFC	allyn.tennant@msfc.nasa.gov
Martin Weisskopf	NASA/MSFC	martin@smoker.msfc.nasa.gov

CXC Coordinator

Belinda Wilkes	CXC Director's Office	belinda@head.cfa.harvard.edu

CXC Contact Personnel

Director:	Harvey Tananbaum	Calibration:	Christine Jones
Associate Director:	Claude Canizares	Development and Operations:	Dan Schwartz
Manager:	Roger Brissenden	Mission Planning:	Bill Forman
Systems Engineering:	Jeff Holmes	Science Data Systems:	Jonathan McDowell
		Deputy:	Mike Nowak
Data Systems:	Pepi Fabbiano	Director's Office:	Belinda Wilkes
Education & Outreach:	Kathy Lestition	Media Relations:	Megan Watzke

Note: E-mail address is usually of the form: <first-initial-lastname>@cxc.harvard.edu
(addresses you may already know for nodes head.cfa.harvard.edu or cfa.harvard.edu should work also)

Status of the Chandra Source Catalog Project

The *Chandra* Source Catalog (CSC) project recently reached a significant milestone, completing a science review conducted by an international committee of experts in X-ray astronomy and astronomical catalog construction. The committee described the development of the *Chandra* Source Catalog as "an important, useful, and exciting project" that is in addition "blazing a path for other facilities."

The CSC will be the definitive catalog of all X-ray sources detected by the *Chandra* X-ray Observatory, and is intended to provide simple access to *Chandra* data for individual sources (or sets of sources matching user-specified search criteria) to satisfy the needs of a broad-based group of scientists, including those who may be less familiar with astronomical data analysis in the X-ray regime. For each X-ray source, the catalog will list the source position and a detailed set of source properties, including commonly used quantities such as source dimensions, multi-band fluxes, and hardness ratios. In addition to these traditional elements, the catalog will include additional source data that can be manipulated interactively, by the user, including images, event lists, light curves, and spectra for each source individually from each observation in which a source is detected.

Design Goals

The primary design goals for the CSC are to (1) allow simple and quick access to the best estimates of the X-ray source properties and *Chandra* data for individual sources with good scientific fidelity, and directly support medium sophistication scientific analysis on the individual source data; (2) facilitate easy searches and analysis of a wide range of statistical properties for classes of X-ray sources; (3) provide a user interface that supports searching and manipulating the actual observational data for each X-ray source in addition to the tabular properties that are recorded in the catalog; and (4) include all real X-ray sources detected down to a predefined threshold level in all of the public *Chandra* datasets used to populate the catalog, while maintaining the number of spurious sources at an acceptable level.

Catalog Releases, Characterization, and User Interfaces

The CSC will be released to the user community in a series of increments with increasing capability. The first release of the catalog is expected to include a subset of the elements described here. Each release of the catalog, including the first, will be accompanied by a detailed characterization of the statistical properties of the catalog to a well defined, high level of reliability. Key properties that will be characterized include limiting sensitivity, completeness, false source rates, astrometric and photometric accuracy, and variability information.

Both the tabulated source properties and the individual pointed observation source data (source images, event lists, etc.) that comprise the CSC will be stored in the *Chandra* Data Archive. The former will be recorded in SQL databases, and the latter will be stored as FITS files. Using this approach leverages existing archive software and provides a file-based interface that is compatible with existing CIAO tools. To ensure traceability, a history of updates will be maintained so that the state of the database at any point in time is recoverable.

The contents of each catalog release will be carefully controlled. They will include the subset of sources extracted from the database that pass quality assurance checks and conform to the characterization requirements established for the release.

Access to the catalog will be provided in two ways. First, a graphical user interface will be provided that will allow users to peruse the catalog, perform queries on real or virtual columns, display results, and download data files. The user interface will comply with published Virtual Observatory standards such as SIAP, VOTable, and ADQL. Second, an application programming interface will provide direct access to the catalog and data from users' data analysis scripts. Such scripts will be able to query the catalog, directly download data, and manipulate the data to perform further searches. The first release of the catalog is expected to include a simplified user interface that does not include all of the capabilities described here.

Catalog Construction

Each pointed observation may include data for tens to hundreds of X-ray sources within the field of view. In addition to recording tabular catalog information about each source individually, the design goals mandate that the actual observational data for each source individually be extracted from each pointed observation that includes that source, and be accessible through the catalog.

The bulk of the CSC construction will be performed by a set of CXC Data System processing pipelines that run using the same automated processing (AP) infrastructure that is used to run standard data processing. For performance reasons, the compute-intensive pipeline processing will be done on a multi-node Beowulf cluster running Linux, and the AP infrastructure has recently been modified to support this capability. Most of the catalog processing steps are performed using existing CIAO data analysis software, although several new tools have been or are being developed for certain tasks that cannot be done using the current CIAO tool set. These new tools will be included in future CIAO releases.

Catalog construction is conceptually a two part process. First, the observational data for each non-proprietary pointed observation is processed to identify the X-ray sources and extract the per-source data and source properties. Second, the source properties for each source that is detected in more than one pointed observation must be reconciled.

Pointed Observation Pipeline Processing

Processing the data from each pointed observation is performed in two steps. The first step handles the data for the entire field of view, detects sources and extracts data for each source for further processing. The second step processes the data for each detected source and extracts the source properties that will ultimately be merged into the master catalog.

The Detect Sources Pipeline reprocesses each pointed observation using a defined set of calibrations and processing algorithms. Full field exposure maps and background maps are generated, and sources are detected in several energy bands. Source and background regions for each detected source are determined for use in the subsequent Per-Source Pipeline.

The Per-Source Pipeline executes for each detected source. The pipeline extracts the photon events in the rectangle bounding the background region for the source, and construct a "postage stamp" image of the region together with a full resolution exposure map and an image of the point spread function (PSF) at the source position. Various spatial, spectral, and temporal source properties are extracted at this point, both directly from the data, and by performing model fitting (for example, fitting the PSF to the postage stamp image) where appropriate.

Merge Pipeline Processing

The main functionality of the Merge Pipeline is to take the source properties extracted from each pointed observation in which the source is detected and merge them together for inclusion in the catalog. The pipeline first performs a cross-match to determine if the source was detected in any other pointed observations. If no matches are found, then the new source properties are promoted. However, if one or more candidate matching sources are found, then the Merge Pipeline must identify which of those candidates match the current source. There is not a one-to-one relationship primarily because the *Chandra* PSF varies significantly across the field of view. Once matching sources are identified, the source information is updated by merging the source properties from the contributing pointed observations based on a set of merging rules.

Ian Evans for the *Chandra* Source Catalog project team

Gregory-Loredo Variability Algorithm for Chandra Data

Reprinted by permission from *ADASS XV Proceedings* (Escorial, Spain, 2005) ASP Conf. Ser., G. Gabriel, C. Arviset, D. Ponz, and E. Solano, eds.

Introduction

We describe using the Gregory-Loredo algorithm (Gregory & Loredo 1992) to detect temporal variability in sources identified in the CXC L3 pipeline (Evans et al. 2006), based on the event files. Briefly, N events are binned in histograms of m bins, where m runs from 2 to $m_{\max}$. The algorithm is based on the likelihood of the observed distribution $n_1\ n_2, ..., n_m$ occurring. Out of a total number of m^N possible distributions the multiplicity of this particular one is $N!/(n_1!\ .\ n_2!\ .\ ...\ .\ n_m!)$. The ratio of this multiplicity to the total number provides the probability that this distribution came about by chance. Hence the inverse is a measure of the significance of the distribution. In this way we calculate an odds ratio for m bins versus a flat light curve. The odds are summed over all values of m to determine the odds that the source is time-variable.

The method works very well on event data and is capable to deal with data gaps. We have added the capability to take into account temporal variations in effective area. As a byproduct, it delivers a light curve with optimal resolution.

Although the algorithm was developed for detecting periodic signals, it is a perfectly suitable method for detecting plain variability by forcing the period to the length of the observation.

Implementation

We have implemented the G-L algorithm as a standard C program, operating on simple ASCII files for ease of experimentation. Input data consist of a list of event times and, optionally, good time intervals with, optionally, normalized effective area. Two output files are created: odds ratios as a function of m and a light curve file.

If m_{max} is not explicitly specified, the algorithm is run twice. The first time all values of m are used, up to the minimum of 3000 and $(t_e - t_b)$ /50; i.e., variability is considered for all time scales down to 50s, which is about 15 times the most common ACIS frame time. The sum of odds $S(m) = \sum O(i) / (i - m_{min} + 1)$, where $i = m_{min} ... m$, is calculated as a function of m and its maximum is determined. Then the algorithm is run again with m_{max} set to the highest value of m for which $S(m) > \max(S) / \sqrt{e}$. In addition to the total odds ratio O the corresponding probability P of a variable signal is calculated.

The light curve that is generated by the program essentially

consists of the binnings weighed by their odds ratios and represents the most optimal resolution for the curve. The standard deviation σ is provided for each point of the curve.

There is an ambiguous range of probabilities: $0.5 < P < 0.9$, and in particular the range between 0.5 and 0.67 (above 0.9 all is variable, below 0.5 all is non-variable). For this range we have developed a secondary criterion, based on the light curve, its average σ, and the average count rate. We calculate the fractions f_3 and f_5 of the light curve that are within 3σ and 5σ, respectively, of the average count rate. If $f_3 > 0.997$ AND $f_5 = 1.0$ for cases in the ambiguous probability range, the source is deemed to be non-variable.

Finally, the program assigns a variability index (see Table 3).

Test Results and Analysis

The program was run on all 118 sources found by the program *wavdetect* in *Chandra* ObsId 635. The total time span of the observation was 102 ks and the sources varied between 5 and 24000 counts. The average time to run the program was 1.5 s per source. 71 sources were found to be variable with an odds ratio > 1.0 (probability > 0.5). Visual inspection of the light curves of all 118 sources found 54 that are variable, though there are a few borderline cases on either side of the divide.

Analysis

Table 3 summarizes the number of variable sources detected, the false, and the missed detections, as a function of odds ratio and probability range.

Using G-L just by itself is problematic in the probability range 0.5-0.9, considering the required trade-off between missed detections and false detections. We solved this problem, as described above, by designing the secondary criterion that is based on the fraction of the light curve within 3σ and 5σ. The final result is that three borderline variable sources are missed (with emphasis on borderline), but there are no spurious detections. However, any user who is concerned about missing potential candidates should be encouraged to inspect all sources with a variability index greater than 0.

The G-L algorithm, as expected, is pleasantly insensitive to the shape of the light curve.

The light curves (and the 3σ curves), in providing precisely the desired resolution, are of the kind that we would want to include in the product package.

Figs. 24 - 26 provide a typical cross-section of the different types of cases. Dashed lines represent the 3σ curves. Fig. 27 shows one of the cases that cannot very well be handled by simple statistics: it fails all criteria, but there appears to be a definite trend; however, we do not consider the source variable.

The tests have also brought to light the issue of time-variable exposure (or effective area). It appears in a number of sources with characteristic times that are harmonics of one of *Chandra*'s two dither periods (707 and 1000 s). Our tests show that this can be properly taken care of by providing the program with normalized effective area as a function of time.

Variability Index	Condition	Comment
0	$0 < P < 0.5$	Definitely not variable
1	$0.5 < P < 0.67$ and $f_3 > 0.997$ and $f_5 = 1.0$	Not considered variable
2	$0.67 < P < 0.9$ and $f_3 > 0.997$ and $f_5 = 1.0$	Probably not variable
3	$0.5 < P < 0.6$	May be variable
4	$0.6 < P < 0.67$	Likely to be variable
5	$0.67 < P < 0.9$	Considered variable
6	$0.9 < P$ and $O < 2.0$	Considered variable
7	$2 < O < 4$	Considered variable
8	$4 < O < 10$	Considered variable
9	$10 < O < 30$	Considered variable
10	$30 < O$	Considered variable

TABLE 3: Variability index.

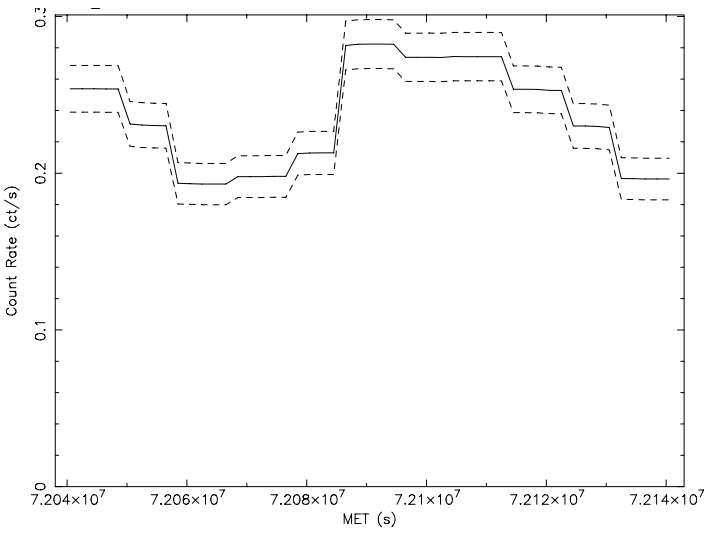

FIGURE 24: Source 3 (24093 counts). Even though the SNR is high, the resolution of the light curve is fairly low since higher resolution is not warranted by its shape.

Odds ratio range	Probability range	Good detections	False detections	Missed with secondary criterion	False with secondary criterion
1.0 - 2.0	0.5 - 0.67	2	7	1	0
2.0 - 9.0	0.67 - 0.9	5	10	2	0
> 9.0	> 0.9	47	0	0	0

TABLE 4: Detection results.

Conclusion

We conclude that G-L provides a robust algorithm for detecting temporal variability that is insensitive to the type and shape of variability and that takes properly into account the uncertainties in the count rate, requiring a statistically significant departure from a flat count rate for it to declare variability. The light curves provided by the program appear to be near-optimal for what we intend to present to users. The addition of the secondary criterion results in a reliable test, though careful users may want to inspect the light curves of all sources with a non-zero variability index.

This work has been supported by NASA under contract NAS 8-03060 to the Smithsonian Astrophysical Observatory for operation of the Chandra X-ray Center. I gratefully acknowledge many useful discussions with Dr. Gregory.

Arnold Rots

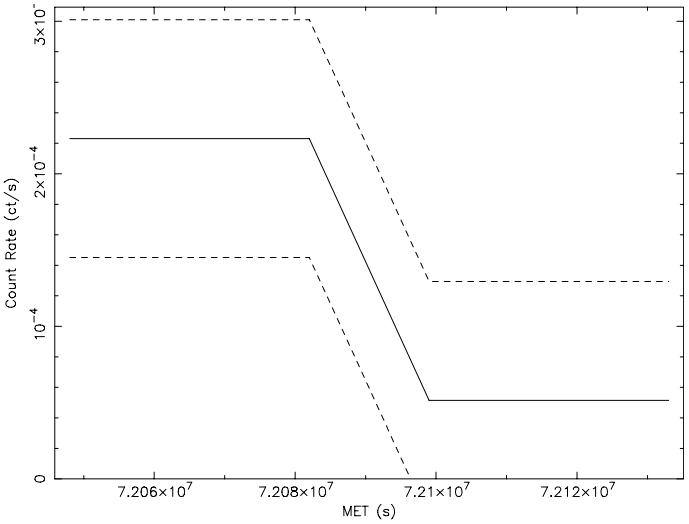

FIGURE 26: Source 110 (14 counts). A low count rate, but variable, nevertheless.

References

Evans, I. et al. 2006, ADASS XV
Gregory, P. C. & Laredo, T. J. 1992, ApJ, 398, 146

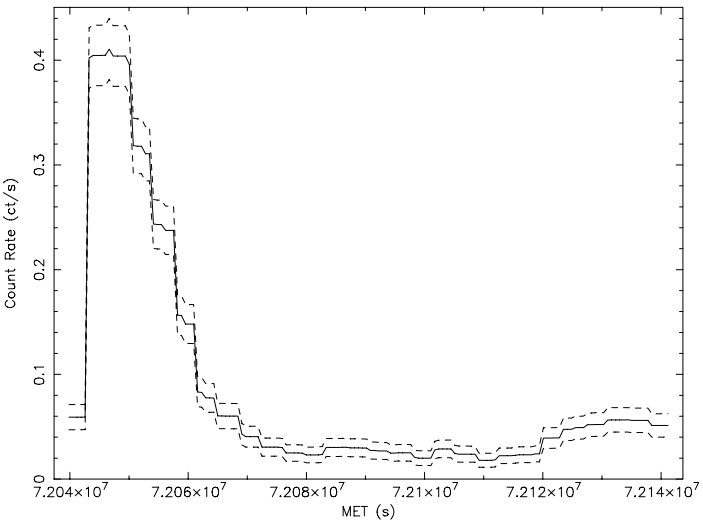

FIGURE 25: Source 11 (8697 counts). The timescale of the changes in this source are very much shorter than in source 3; hence the resolution is higher.

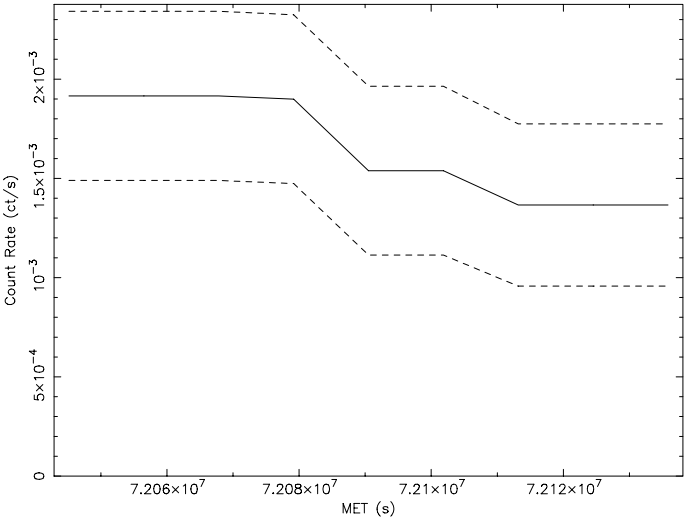

FIGURE 27: Source 25 (170 counts). This is an example of a borderline case where there is no statistically significant change while there is yet an unmistakable trend. I still would not consider this source variable.

Angels and Dragons: On Handling Systematic Error

At the end of the *Chandra* Calibration Workshop on Nov 1, 2005 a special session was held that focused on calibration uncertainties and their effect on data analysis. It was clear during the session that astronomers have a love/hate relationship with systematic errors. As Steve Snowden put it, "Here there may be dragons," and Dick Edgar quoth, "Systematic Errors are like angels." All the presentations are available on-line at http://cxc.harvard.edu/ccw/proceedings/05_proc/ - not only will you find more details here, including plots of the data and compelling expositions of instrumental effects, but also a rewrite of a Far Side cartoon that is destined to be a classic.

Context: What is Systematic Uncertainty?

Dragons

Astronomers and physicists are in a special position as far as what we call "systematic uncertainties", or calibration errors, go. To an astrophysicist, these are errors inherent in modeling the instrument (telescope and subsystems). They are not the same as "bad measurements" such as cosmic ray hits, dead pixels, and other physical outliers. They affect accuracy. Unknown, these errors can produce systematically biased results as well as smearing. Hence Steve Snowden's description of unmapped problems: "Here There Might Be Dragons".

Angels

On the other hand, compared to other fields, we can specify our sources of error to an extraordinary degree. Elsewhere (e.g., social sciences, or economics [*Ed:* aren't they the same?]), one models or fits a non-specific extra variance along with the scientific theory. In contrast, we measure them ahead of time, each in specific detail. Once found, we investigate their physical cause. Though each case is different, we have a rough idea of the unique distribution of each, however complex. Thus Dick Edgar's aphorism: "Systematic errors are like angels. They are not a single breed; they are individually created." However we have not yet developed techniques that incorporate that information in the analysis.

Generalizing

Statisticians use the term "Model Mismatch" where astronomers and physicists use "systematic uncertainties". One sees that these broad terms incorprate uncertainties ranging from calibrating our intruments (e.g., HETG energy scale, HRMA effective area, ACIS response) and backgrounds, to calibrating our underlying physics (e.g., atomic lines database). All these topics are represented here. Whenever there is a model-mismatch that affects one's astrophysical inference, there is a bias in the inference. Once it is mapped, it becomes known physics or well-understood instrumental features.

Work

What effect does our model mismatch have on our final results? How do we incorporate it in a rigorous but sensible (i.e. reasonably fast and uniform) way? In the past, researchers have often assumed these uncertainties could be added in quadrature as if they were uncorrelated Gauss-Normal errors. However, calibration errors are often correlated, non-Gaussian, and asymmetric, and many speakers (and statisticians) emphasized that Gaussian assumptions are incorrect.

Here Be Dragons

The Soft X-Ray Background

Brad Wargelin and Steve Snowden emphasized the effects of the astrophysical X-ray background. Brad's main point: It varies! It varies in time and space. It varies with solar cycle. There is a geocoronal soft X-ray glow, which is usually weak, but can have bright `Solar Gusts'. It varies due to charge exchange, from solar wind ions colliding with neutral gas in the heliosphere and the Earth's outer atmosphere. The charge exchange energy spectrum is all below ~1.5 keV, with most of the X-ray emission from He-like and H-like O. Its spatial distribution is complex, with the highest intensities observed when looking near the Sun and/or toward the Galactic Center through the helium focusing cone. Users should know these places: "Here there might be dragons!" It particularly affects measurements of extended sources: SXRB, clusters, etc.

High Angular Resolution Imaging

Although the *Chandra* Point Spread Function (PSF) is encouragingly well-known on axis, and near the peak, don't forget the "dragons" in the wings! The PSF varies tremendously as a function of off-axis angle and photon wavelength (energy). Margarita Karovska showed many examples of the *Chandra* PSFs and described the variations in it. There are subtle differences in measured the image for sources at different distances from the image center; for example, could it be a double source or a single point source with the PSF "splitting" it into an apparent double? How much of the emission is due to extended sources, and how much to wings of PSF?

A scary thought: we know our knowledge of PSF is incomplete, especially in the wings. So by what procedure does the researcher decide what to publish?

An aside: the various deconvolution methods in common use (Richardson-Lucy, simple Maximum Entropy, the new multiscale EMC2) can all be understood as 'forward fitting' function with flexible non-parametric or semi-parametric models (i.e. based on

likelihood of these kinds of models of the sky convolved with instrument response). So such methods have a wealth of statistics frameworks behind them. The EM algorithm Richardson-Lucy, essentially, uses a model for the sky that is independent pixels on the sky. This can work nicely for clusters of point-sources; but not as well for smooth diffuse emission, as it effectively models only one scale (pixel size). The EMC2 method (which does not yet include PSF variations) incorporates a Haar-wavelet-like multiscale model, which essentially can add some smoothing. It is a better choice for modeling diffuse emission.

Taming the Dragon

Parametric Estimation Analysis

Jeremy Drake looked at how to get a handle on correlated uncertainties that arise from the accumulated calibration errors from various components of the subassembly instrument modules that contribute to the instrument effective area (ARF). He obtained a large sample of these ARFs (specifically, for the ACIS-I) and carrying out model fits to the same dataset for each of these ARFs, he derived an estimate of the stability of the model parameters to the calibration error. Variations in the ARF can be seen in systematic shifts in inferred values of astrophysically interesting model parameters. Though often small, one sometimes sees "surprising pathologies".

Fitting the same source spectrum hundreds or thousands of times with differing ARFs is however impractical for the average user. Hence a 'compressed', more elegant and efficient representation of these variations is called for.

Dimensionality Reduction

This is Rima Izem's (a statistician) simple-sounding title for an elegantly simple method to 'encode' the correlated calibration uncertainties in order to be able to incorporate them into practical fits. Thousands of simulated curves, each with ~1000 energy bins, is too much to handle simply. However, continuous functions (such as the simulated ACIS ARFs used by Jeremy) are nicely expressed as basis functions in the form of principal components of the functional variations. Astrophysicist are probably more familiar with looking for principal components (that is, directions of maximum variation, or eigenvectors) as directions in a point-cloud. There is an analogy for function space: consider each energy bin of the ACIS ARF curves as a separate dimension, and perform the PCA analysis there. Mapping back to function-space gives curves reflecting the maximum variations in the data. Their associated eigenvectors describe the amount of variation each curve is responsible for. The compression achieved with this method is phenomenal. The ~1000 simulated curves describing a complex correlated functionals of the ACIS ARF could be described almost entirely with ~5 components.

With this elegant and compact representation, one can reasonably include calibration uncertainties in one's analyses in a practical way. It still requires a robust method such as Markov-Chain Monte Carlo to search the parameter-space to do the fit. It is also generalizable to higher dimensions, such as the instrument energy response function (RMF) and/or PSF.

Here Be Angels

Some dragons have been slain. Or at least tamed. Or rather, doused. Temporarily.

Pixel Randomization

The practice of pixel randomization, where a uniform random deviate is added to the photon detector positions in order to reduce residual aspect-related errors and improve the astrometry, came in for much criticism. Herman Marshall argued that while it may be a good practice for diffuse or large sources, it is a bad idea for point sources. It is easy to show graphically that randomization ends up broadening the PSF (not a surprise).

The Advantages of User Collaboration With the Calibration Team

Randall Smith appealed to the users to "please work with the calibration team!" First check if you can make suitable corrections for your data, rather than wait for the calibration team to notice the problem and come up with fix. After all, users would know what to look for, because they are familiar with their data. Randall pointed to some specific cases where user collaboration has significantly improved the magnitude and scope of calibration efforts: micro-roughness affecting the off-axis PSF, pixel randomization in grating data, the ACIS chips contamination problem, etc. "Users, please work with the calibration team! It will get done faster and better; and be a service to the community."

Atomic Data Uncertainties

Strictly speaking, this falls more in the realm of model uncertainties than calibration uncertainties, but the effects are similar. Nancy Brickhouse pointed out that only a few laboratory measurements of astrophysically interesting lines exist, and there are so many lines that theoretical estimates are unavoidable. In addition, there are lines missing from atomic database compilations, including missing satellite lines, as well as missing processes that contribute to the intensity of a line. So there are a large number of systematic unknown uncertainties which are *not* random, and for which errors *should not* be added in quadrature. Systematic model mis-match errors are likely to be more important than statistical error in these cases and sensitivity testing is essential. The ATOMDB database (http://cxc.harvard.edu/atomdb/) from APEC includes errors on individual lines, so now there is an opportunity to test out different approaches.

Propagation of Background Uncertainties into Cluster Temperature

A cluster is a large diffuse source, so typical background estimation methods (e.g., taking a small annular aperture around the source) are not useful. Maxim Markevitch deals with this prob-

lem by deriving a robust model for the background. Starting with the simplest case for understanding the background, i.e., acquiring the quiescent detector background when the detector is covered, he finds that the background is constant. Next, examining the quiescent blank-sky backgrounds at E > 2 keV, he finds that it is simple enough, in this case, to add the E ~ 2 keV background in quadrature. (For details on how to use the ACIS "Blank-Sky" background files, see the CIAO thread on the subject, at http://cxc.harvard.edu/ciao/threads/acisbackground/.) This can be done similarly for XMM though XMM backgrounds are less predictable, usually due to flares.

Missing Lines, Calibration Errors, or What?

Ooops! Jürgen Schmitt found dramatic differences between plus and minus orders in the MEG grating spectrum of the bright flare star AU Mic. This was easily explained (after considerable work) as simply statistical fluctuations at play. His advice: "Always go back to the raw data."

We Are All In This Together

As Herman Marshall emphasized, we must develop an "Experience Database," with both the calibration team and the users providing their input. One needs both physics-based models as well as semi-parametric phenomenological models; the first gives us a better understanding of the source of the errors, but unlike the latter, is usually computationally more complex. Andy Pollock reiterated that there is a need for some standards in how to report and handle these uncertainties. We should run many more simulations as a regular part of our data analysis, and include our understanding of calibration errors into the results we report. There is also a strong need to develop techniques to include calibration uncertainties in data analysis if a calibration team is providing us with such information.

In summary, a list of take-home points:

1. Interactions with users are very important in the identification and accounting of systematic errors.
2. There is still a large gap between 'theory' and implementation. When is `sensitivity testing' (where we know we don't know) the best we can do? How/when can we do better?
3. Each kind of calibration uncertainty or model mis-match requires careful examination.
4. Even when we (mostly) understand the physics behind the calibration uncertainties, it is still a significant effort to implement this information in a way that is practical.
5. In particular, how does the community make standards for communicating, working with, and updating calibration uncertainties?

Alanna Connors, Vinay Kashyap, and Aneta Siemiginowska

Chandra-Related Meetings Planned for the Next Year

Keep an eye on the CXC Webpage:
http://cxc.harvard.edu for further information

Chandra Users' Committee Meeting
April 5, 2006 Cambridge, MA
http://cxc.harvard.edu/cdo/cuc/index.html

Chandra Fellows Symposium
October, 2006 Cambridge, MA
http://cxc.harvard.edu/fellows/

Chandra Users' Committee Meeting
October, 2006 Cambridge, MA
http://cxc.harvard.edu/cdo/cuc/index.html

Extragalactic Surveys
Chandra Science Workshop
November 6-8, 2006 Cambridge, MA
http://cxc.harvard.edu/xsurveys06/

Previous Chandra-related meetings:

Chandra and Star Formation
July 13-15, 2005 Cambridge, MA
http://cxc.harvard.edu/stars05/

The Fourth X-ray Astronomy School
August 14-19, 2005 Cambridge, MA
http://xrayschool.gsfc.nasa.gov/docs/xrayschool/

Chandra Fellows Symposium
October 11, 2005 Cambridge, MA
http://cxc.harvard.edu/fellows/

Chandra Users' Committee Meeting
October, 2005 Cambridge, MA
http://cxc.harvard.edu/cdo/cuc/index.html

Six Years of *Chandra* Science Symposium
November 2-4, 2005 Cambridge, MA
http://cxc.harvard.edu/symposium_2005/index.html

Chandra Calibration Workshop
October 31 - November 1, 2005 Cambridge, MA
http://cxc.harvard.edu/ccw/

Using the Parallel Virtual Machine for Everyday Analysis

Reprinted by permission from *ADASS XV Proceedings* (Escorial, Spain, 2005) ASP Conf. Ser., G. Gabriel, C. Arviset, D. Ponz, and E. Solano, eds.

Introduction

Parallel computing is not a new discipline, so it is surprising that few astronomers resort to parallelism when solving standard problems in data analysis. To quantify this assertion relative to the X-ray community, in late summer of 2005 we conducted several full text searches of the NASA ADS digital library (Kurtz et al 1993), as follows:

Keywords	Number of Hits
parallel AND pvm	38
message AND passing AND mpi	21
xspec	832
xspec AND parallel AND pvm	0
xspec AND message AND passing AND mpi	0

Extra keywords were included with PVM and MPI so as to cull false matches (e.g. with the Max Planck Institute). The keyword *xspec* refers to the software program of the same name (Arnaud 1996), which is generally regarded as the most widely used application for modeling X-ray spectra. Queries in ADS on other modeling tools, or with other search engines such as Google, all yield similar trends: astronomers and astrophysicists do employ parallel computing, but mainly for highly customized, large-scale problems in simulation, image processing, or data reduction. Virtually no one is using parallelism for fitting models within established software systems, especially in the interactive context, even though a majority of papers published in observational astronomy result from exactly this form of analysis.

ISIS, S-Lang, PVM, and SLIRP

To exploit this opportunity we've extended ISIS, the Interactive Spectral Interpretation System (Houck 2002), with a dynamically importable module that provides scriptable access to the Parallel Virtual Machine (Geist et al 1994). PVM was selected (e.g. over MPI) for its robust fault tolerance in a networked environment. ISIS, in brief, was originally conceived as a tool for analyzing *Chandra* grating spectra, but quickly grew into a general-purpose analysis system. It provides a superset of the XSpec models and, by embedding the S-Lang interpreter, a powerful scripting environment complete with fast array-based mathematical capabilities rivaling commercial packages such as MatLab or IDL.

Custom user models may be loaded into ISIS as either scripts or compiled code[1], without any recompilation of ISIS itself; because of the fast array manipulation native to S-Lang, scripted models suffer no needless performance penalties, while the SLIRP code generator (Noble 2003) can render the use of compiled C, C++, and FORTRAN models a nearly instantaneous, turnkey process.

Parallel Modeling

Using the PVM module we've parallelized a number of the numerical modeling tasks in which astronomers engage daily, and summarize them here as a series of case studies. Many of the scientific results stemming from these efforts are already appearing elsewhere in the literature.

Kerr Disk Line

Relativistic Kerr disk models are computationally expensive. Historically, implementors have opted to use precomputed tables to gain speed at the expense of limiting flexibility in searching parameter space. However, by recognizing that contributions from individual radii may be computed independently we've parallelized the model to avoid this tradeoff. To gauge the performance benefits[2] we tested the sequential execution of a single model evaluation, using a small, faked test dataset, on our fastest CPU (a 2Ghz AMD Opteron), yielding a median runtime of 33.86 seconds. Farming the same computation out to 14 CPUs on our network reduced the median runtime to 8.16s, yielding a speedup of 4.15. While 30% efficiency seems unimpressive at first glance, this result actually represents 67% of the peak speedup of 6.16 predicted by Amdahl's Law (5.5 of the 33.86 seconds runtime on 1 CPU was not parallelizable in the current implementation), on CPUs of mixed speeds and during normal working hours. Reducing the model evaluation time to 8 seconds brings it into the realm of interactive use, with the result that fits requiring 3-4 hours to converge (on "real" datasets such as the long XMM-Newton observation of MCG--6-30-15 by Fabian) may now be done in less than 1 hour. The model evaluation is initiated in ISIS through the S-Lang hook function

```
public define pkerr_fit (lo, hi, par)
{
   variable klo, khi;
   (klo, khi) = _A(lo, hi);   % convert angstroms to KeV
   return par[0] * reverse ( master (klo, khi, par));
}
```

where `lo` and `hi` are arrays (of roughly 800 elements) representing

[1]Usually in S-Lang, but Python may also be used by simply importing the PySL module.

[2]A more complete and rigorous analysis will be presented in a future journal paper.

the left and right edges of each bin within the model grid, and par is a 10 element array of the Kerr model parameters. Use of the PVM module is hidden within the master call (which partitions the disk radii computation into slave tasks), allowing ISIS to remain unaware that the model has even been parallelized. This is an important point: *parallel models are installed and later invoked using precisely the same mechanisms employed for sequential models*.

For each task the slaves invoke a FORTRAN *kerr* model implementation, by Laura Breneman at the University of Maryland, wrapped by SLIRP as follows:

```
linux%  slirp -make kerr.f
Starter make file generated to kerr.mf
linux%  make -f kerr.mf
```

Confidence Contours and Error Bars

Error analysis is ripe for exploitation with parallel methods. In the 1D case, an independent search of χ^2 space may be made for each of the I model parameters, using $N=I$ slaves, with each treating one parameter as thawed and $I-1$ as fixed. Note that superlinear speedups are possible here, since a slave finding a lower χ^2 value can immediately terminate its $N-1$ brethren and restart them with updated parameters values. Parallelism in the 2D case is achieved by a straightforward partition of the parameter value grid into J independently-evaluated rectangles, where $J >> N$ (again, the number of slaves) is typical on our cluster. Our group and collaborators have already published several results utilizing this technique. For example, Allen et al 2004 describes joint X-ray, radio, and γ-ray fits of SN1006, containing a synchrotron radiation component modeled as

$$\frac{dn}{dkdt} = \frac{\sqrt{3}e^3 B}{hmc^2 k} \int dp N(p) R\left(\frac{k}{k_0 \gamma^2}\right)$$

The physics of this integral is not important here; what matters is that the cost of evaluating it over a 2D grid is prohibitive (even though symmetry and precomputed tables have reduced the integral from 3D to 1D), since it must be computed once per spectral bin, hundreds of times per model evaluation, and potentially millions of times per confidence grid. A 170x150 contour grid (of electron spectrum exponential cutoff energy versus magnetic field strength) required 10 days to compute on 20-30 CPUs (the fault tolerance of PVM is critical here), and would scale linearly to a 6-10 month job on a single workstation.

Temperature Mapping

Temperature mapping is another problem that is straightforward to parallelize and for which we have already published results. For instance, Wise & Houck 2004 provides a map of heating in the intracluster medium of Perseus, computed from 10,000 spectral extractions and fits on 20+ CPUs in just several hours.

[1]This also makes it easy for ISIS to employ an MPI module for parallelism, if desired.

Going Forward

It is important to note that in the two previous studies *the models themselves were not parallelized*, so the usual entry barrier of converting serial codes to parallel does not apply. One consequence is that the community should no longer feel compelled to compute error analyses or temperature maps serially. Another consequence is that the independence between partitions of the data and the computation being performed, which makes the use of sequential models possible in the parallel context, also lurks within other areas of the modeling problem. In principle it should be possible to evaluate an arbitrary sequential model in parallel by partitioning the model grid over which it's evaluated, or by evaluating over each dataset independently (when multiple datasets are fit), or in certain cases even by evaluating non-tied components in parallel. We are implementing these techniques with an eye towards rendering their use as transparent as possible for the non-expert. With simple models or small datasets these measures may be not be necessary, but the days of simple models and small datasets are numbered. Reduced datasets have already hit the gigabyte scale, and multi-wavelength analysis such as we describe above is fast becoming the norm. These trends will only accelerate as newer instruments are deployed and the Virtual Observatory is more widely utilized, motivating scientists to tackle more ambitious analysis problems that may have been shunned in the past due to their computational expense.

M.S. Noble, J. C. Houck, J. E. Davis, A. Young, M. Nowak

This work was supported by NASA through the AISRP grant NNG05GC23G and Smithsonian Astrophysical Observatory contract SV3-73016 for the Chandra X-Ray Center.

References

Allen, G. E., Houck, J. C., & Sturner, S. J. 2004, Advances in Space Research, 33, 440

Kurtz, M.J., Karakashian, T., Grant, C.S., Eichhorn, G., Murray, S.S., Watson, J.M., Ossorio, P.G., & Stoner, J.L. 1993 ADASS II

Arnaud, K.A. 1996 ADASS V

A. Geist, A. Beguelin, J. Dongarra, W. Jiang, R. Manchek, & V. Sunderam 1994, PVM: Parallel Virtual Machine, A User's Guide and Tutorial for Networked Parallel Computing

Houck, J. C. 2002, ISIS: The Interactive Spectral Interpretation System, High Resolution X-ray Spectroscopy with XMM-Newton and Chandra

Noble, M. S. 2003, http://space.mit.edu/cxc/software/slang/modules/slirp

Wise, M., & Houck, J. 2004, 35th COSPAR Scientific Assembly, 3997

Where Do the Data Go?
An Analysis of Chandra Data Dissemination

Reprinted by permission from *ADASS XV Proceedings* (Escorial, Spain, 2005) ASP Conf. Ser., G. Gabriel, C. Arviset, D. Ponz, and E. Solano, eds.

Introduction

The *Chandra* Data Archive (CDA) has been distributing data to users since September 1999. Over the years, four interfaces to the archive have been developed: two are web-based; one is stand-alone; and one is ftp-based. The public data in the CDA are mirrored at sites around the world. Downloads are logged, and since 2002 have been maintained in a database (Blecksmith et al. 2003). In addition to tracking the number of files and the volume of data being downloaded, this database is used to perform meta-analyses. Questions addressed in this paper include: (1) At what rate are the applications used relative to each other? (2) Where do users come from? (3) Is there a link between where a user is from and which application is used? (4) What sorts of events trigger downloads of a particular observation?

Relative Application Use

Users can connect to the CDA and browse or retrieve data using a number of interfaces. At this time no single interface provides access to all classes of data in the archive. As a result, all analyses include only downloads that can be done through WebChaser which has the smallest set of retrievable products. As a result, in this study we count only downloads of public data, excluding engineering observations and supporting products.

Provisional Retrieval Interface (PRI):

The original interface to the CDA providing access to public data, it is a CGI script with minimal search capabilities. It is the only GUI-based interface providing access to engineering observations.

Chaser:

This is a stand-alone Java application providing access to proprietary as well as public data. Users can enter individual selection criteria, as well upload criteria from a file. Search results may be viewed in Chaser or saved to a file. Users may select individual files which may be downloaded directly or staged to an ftp area. Chaser is the only interface providing access to supporting products.

WebChaser:

This is a web-based application providing access to proprietary and public data. Search criteria must be entered individually, but WebChaser provides the most detailed search results, including quick-look images, V&V reports, and links to processing status and publications tracked by the CDA operations group. Primary and secondary data packages are downloaded to an ftp staging area.

FTP:

This is an anonymous ftp-site holding primary and secondary products for all public observations.

An analysis of downloads shows that the choice of application depends upon the number of observations downloaded. Most sessions result in fewer than 10 downloaded datasets. When

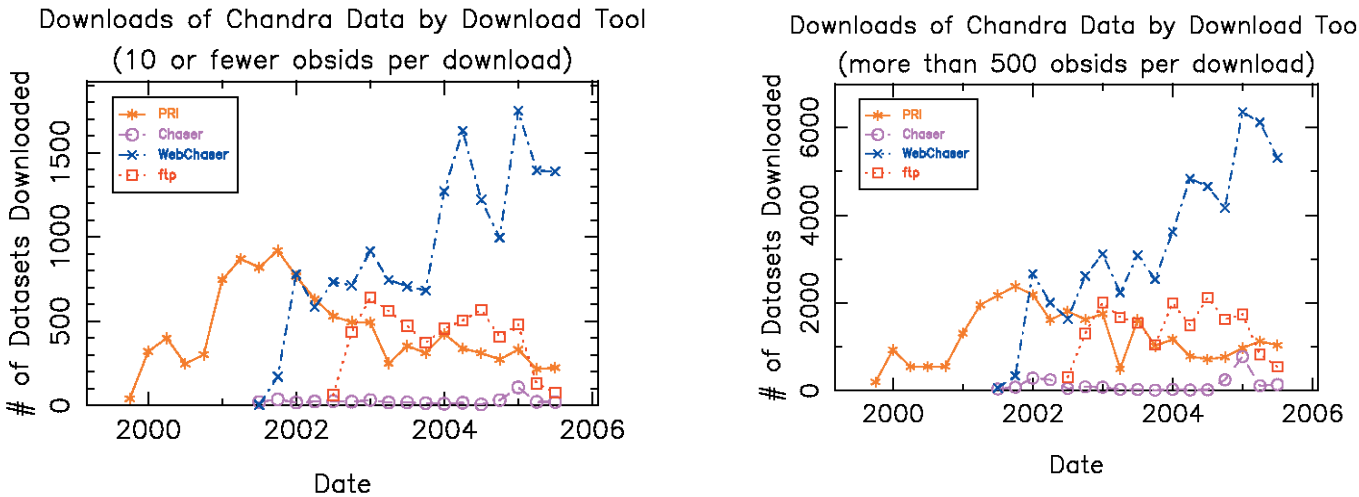

FIGURE 28: Relative download application use for downloads of 10 or fewer and of 500 or more datasets in a three month period by a single host.

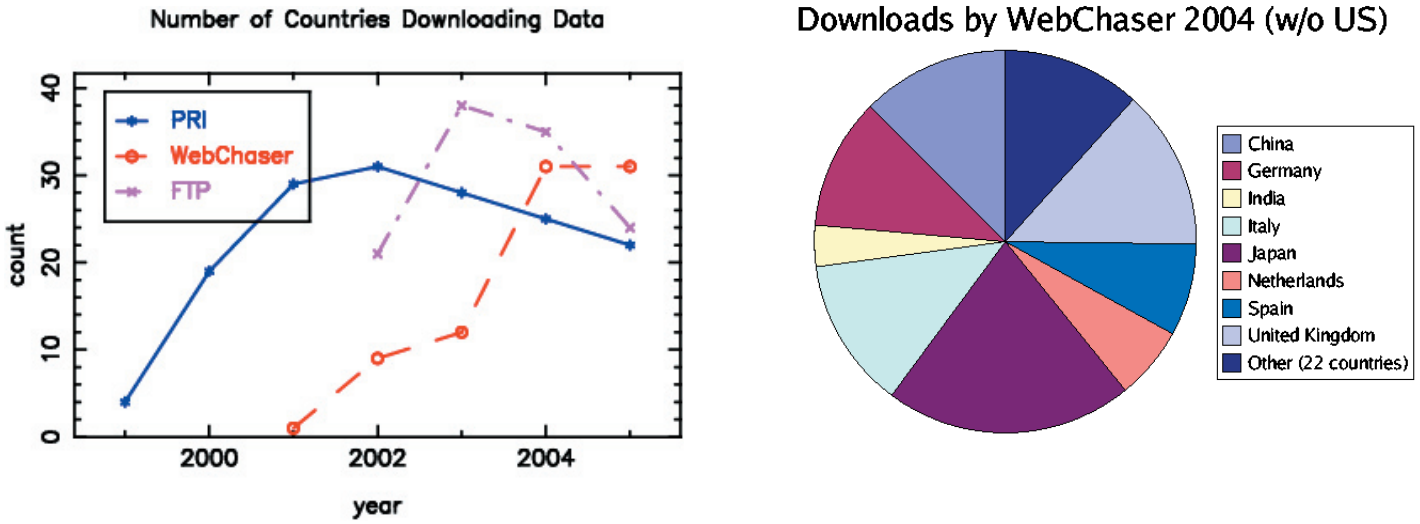

FIGURE 29: Left: Percentage of *Chandra* downloads by country for PRI, FTP, and WebChaser. Right: Relative downloads by country for WebChaser in 2004.

Chaser and WebChaser came on-line in mid-2001, the usage of the PRI began a steady decline, however a not insignificant number of users continue to use it today. Chaser's predominant use is to download supporting products. For large downloads (more than 500 observations per download) users prefer the FTP site. For smaller downloads, most users prefer WebChaser and users have a slight preference for the FTP site over the PRI.

User Demographics

While the vast majority of CDA users are from the United States, we see a steadily increasing number of countries accessing the archive each year. We've gone from serving 22 countries in 2000 to 40 countries in 2004 and have served 57 countries through the course of the mission. Several countries download significant volumes of data; some of these either host or are scheduled to host mirror-sites of the public data. The data show China in particular to be a major user of the CDA, making it a good candidate for a future mirror site.

It is interesting to note there are country specific preferences for accessing the CDA. For instance, the majority of users in the UK prefer WebChaser while users in Japan prefer FTP. This may be related to the UK becoming a mirror site host in 2002, which improves response time for local use of WebChaser. Japan is scheduled to host a mirror site in the near future, which should hopefully make the use of WebChaser with its superior search capabilities more attractive. Users in China seem to prefer the PRI (with the exception of 2004, when there were two complete downloads of the archive using ftp). The PRI, a much

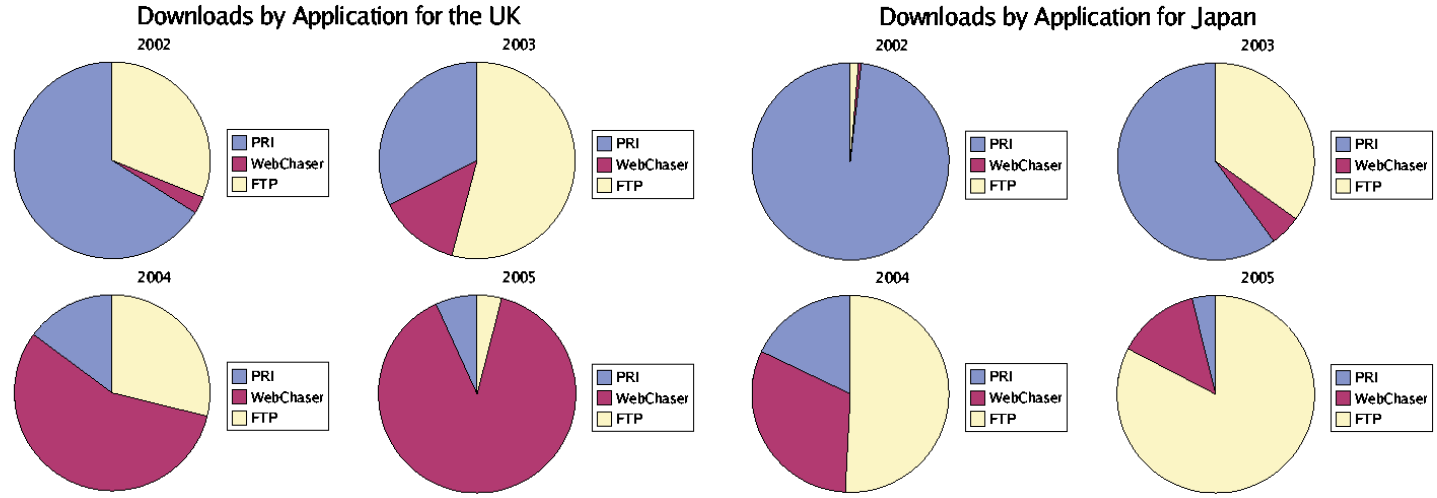

FIGURE 30: Relative usage of PRI, WebChaser, and ftp for the UK and Japan.

simpler application than WebChaser, requires much less network bandwidth and thus may be more appealing in countries with limited bandwidth.

Publications and Downloads

What sorts of events trigger downloads of a particular observation? Three obvious events are the public release of data (the date of which is available in the CDA), scientific publication of the data (tracked by the CDA operations group (Rots et al. 2004)), and media coverage related to the observation (tracked by the *Chandra* Education and Public Outreach group). We find that, not surprisingly, all three types of events increase the number of downloads. Most observations are downloaded within days of going public, indicating that users monitor the archive for such events. Scientific publications increase downloads around the time of the publication, more so for the first publication associated with an observation. Press releases have a lesser effect, stimulating downloads only if the release is picked up by many large media services.

Conclusion

Our analysis of the *Chandra* downloads database indicates that users generally prefer web interfaces and direct access via ftp to stand alone applications. Preferences for download applications vary by country, possibly because of varying bandwidth. Public release of a dataset, scientific publications of data, and major press coverage all appear to increase the downloads of an observation near the time of the event.

This work is supported by NASA contract NAS 8-03060.

S. Winkelman, A. Rots, A. Duffy, S. Blecksmith, D. Jerius
Chandra X-ray Center/Smithsonian Astrophysical Observatory

References

Blecksmith, E., Paltani, S., Rots, A. & Winkelman, S. 2003, adassxii, 283
Rots, A., Winkelman, S., Paltani, S., Blecksmith, S. & Bright, J. 2004, adassxiii, 605

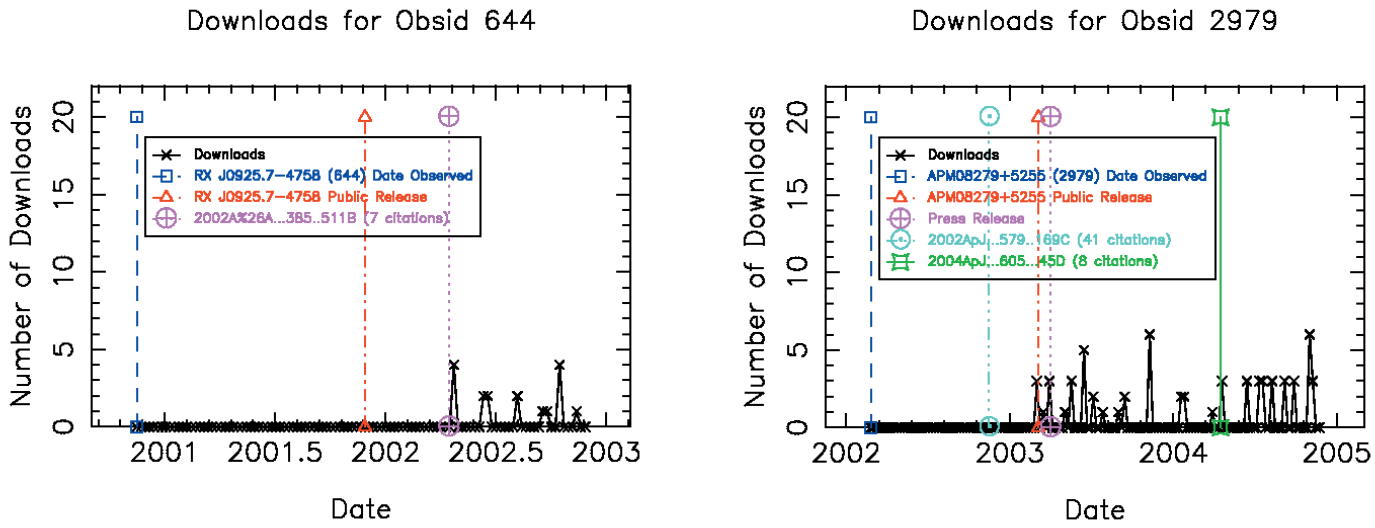

FIGURE 31: Time-lines of two *Chandra* observations showing the effects of public release, scientific publications and media coverage on downloads.

News From The Chandra Data Archive

In the previous issue of the *Chandra* Newsletter we announced a new feature in manuscript preparation: the inclusion of Dataset Identifiers to provide links between the literature and the data. Since then we have updated our informational web page on these identifiers with a tool that provides users with tools to determine the correct syntax of all existing Dataset Identifiers and to request the assignment of custom Dataset Identifiers for large groups of ObsIds.

Since early October users in south Asia are being served public *Chandra* data from a mirror at IUCAA in Pune, India. All browse functions in WebChaser and FastImage still go through our servers at CfA/CXC, but when users request the retrieval of data, their geographic location is determined and, if in southern Asia, the data are prepared at the Pune mirror, rather than in Cambridge, MA. Note that this only applies to primary and secondary products for public data; proprietary data are still exclusively retrieved from the archive at CfA/CXC.

We hope that this will speed data transfers for our users in the region and encourage them to give it a try, especially if they have been reluctant in the past due to low transmission speeds. HEASARC, at GSFC/NASA, has a similar mirror which feeds retrievals through its Browse interface. We are planning to establish several of these mirrors around the globe.

Arnold Rots
for the Archive Operations Team

The Six Years of Science with Chandra Symposium

During three beautiful sunny days in November 2005 more than 270 astronomers from all over the world traveled to Cambridge for a symposium which highlighted scientific results from the the six years of operations of the *Chandra* X-ray Observatory which was launched on July 22 1999. Some of the recent results from the XMM-Newton Observatory were also reported during the meeting.

The symposium was dedicated to Leon Van Speybroeck, the *Chandra* telescope scientist who designed the *Chandra* mirrors. In his honor Dr. Paul Reid from the CfA presented a review talk entitled "X-Ray Optics: past, present and future" where he discussed the development of X-ray optics for astronomy recounting some of the technical problems, solutions, and lessons learned in fabricating the optics for the *Einstein* and *Chandra* Observatories. He also reviewed new ideas for future new X-ray telescopes. In his last slide he summarized Leon's contribution to X-Ray astronomy using these words: *"This talk is dedicated to the memory of Leon Van Speybroeck without whom neither would I be here talking to you nor would Chandra be the exquisite Observatory it is."*

Twelve other invited talks, 39 contributed talks and 156 posters were presented during the meeting in all subjects of X-ray astronomy from solar system to cosmology. A few graduate students and young postdocs (plus a couple of less young ones!) responded to the invitation of advertising their poster in a 1-minute oral presentation. Some of these quick highlights really captured the essence of the posters and one of the most memorable ones was even presented as a "Seussian" sonnet by Ryan Hickox (CfA):

The cosmic X-ray background, it has recently been shown
Comes from mostly AGN and sources that are known

And so it seems the problem is quite close to being solved
But still there is a bit of flux that remains unresolved

Using data from the Chandra Deep Fields North and South, of course
We find the unresolved flux, excluding every source

The hardest part is taking care of backgrounds in the ACIS
But after that subtraction, still some flux remains, in traces

Quite significant a signal, it is larger than you'd guess
From a quick extrapolation of the known logN/logS

And so there still remains an X-ray background mystery
Are there lots of fainter sources? are they starburst galaxies?

If you'd like hear about all this analysis and more
Then please do come along by poster number 4.4

A special session entitled "Enhancing *Chandra* Images for Publication and Public Outreach" was organized by the *Chandra* Education & Public Outreach (EPO) group during one lunch break. It was a very informative session during which we all learned new tips & tricks for preparing *Chandra* images suitable

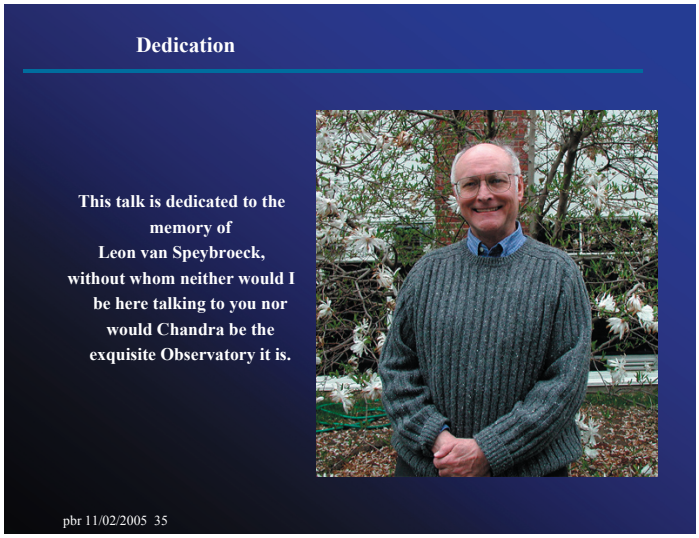

FIGURE 32: The symposium dinner was held at the Museum of Science, where participants reminisced about Leon and enjoyed the exhibits. Clockwise from upper left: a. Harvey Tananbaum shares stories. b. Harvey Tananbaum with Leon's wife Erin, daughter Elaine, and son David. c. Antonella Fruscione. d. Paul Reid's final slide.

for a wide range of publications.

Aside from the wealth of interesting and new scientific results, one of the social highlights of the symposium was the dinner held at the Boston Museum of Science. During the event Harvey Tananbaum, Steve Murray, Gordon Garmire, Martin Weisskopf and Claude Canizares remembered in short speeches their colleague and friend Leon. Leon's wife and two of his children were special guests both at the dinner event and at Paul Reid's talk. Following the dinner an eager crowd was invited to a private viewing of the museum's special exhibit Star Wars: Where Science Meets Imagination. (Figure 32)

Several photographs from the symposium and the dinner event can be found one line at
http://cxc.harvard.edu/symposium_2005/photographs
Also on-line are the symposium proceedings at
http://cxc.harvard.edu/symposium_2005/photographs/
Conference materials will be linked to the ADS in the near future.

To conclude here is a nice e-mail of appreciation from one of the participants:

"I really enjoyed the symposium last week. Most of the talks contained enough tutorial material so a listener who was not a specialist in that area could learn. At least I did. It may have been choice of speakers or instructions to speakers but the final result was very good. I also liked having posters up for several days. There was finally time to read them. The hotel was a nice choice and the meeting seemed to progress smoothly. Congratulations to both scientific and administrative organizers!"

See you at the Eight Years of Science with Chandra Symposium in 2007!

Antonella Fruscione
Six Years Symposium Chair

X-ray Astronomy School 2005

The 4th International X-ray Astronomy School, sponsored by the *Chandra* X-ray Center and NASA Goddard Space Flight Center, was held in Cambridge, MA on August 15-19, 2005. The X-ray Astronomy school is held every other year and is intended for graduate students and recent postdocs who want to understand the intricacies of X-ray astronomy. Emphasis is placed on the foundations of X-ray astronomy rather than on any particular software tools. The lectures presented at the recent school covered a broad range of X-ray astronomy topics including characteristics of X-ray detectors, techniques used to analyze the data and recent advances in several fields of X-ray astronomy, e.g. stars, galaxies,

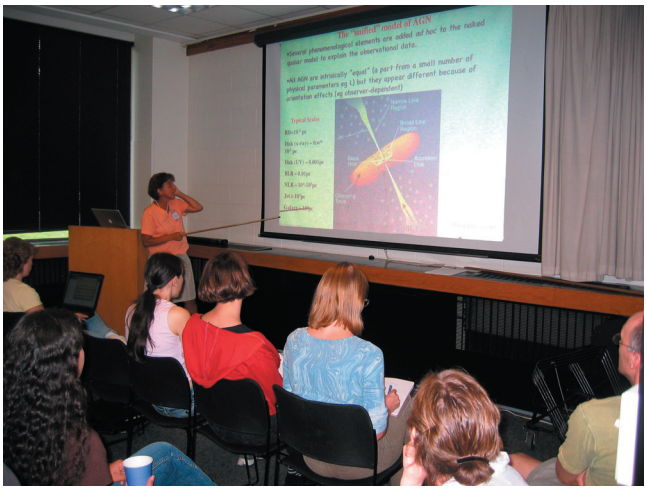

FIGURE 33:Antonella Fruscione presenting ``An Introduction to Active Galactic Nuclei in the X-rays''

AGNs and clusters of galaxies.

48 students attended the school. Morning sessions were devoted to classes and lectures, while the afternoons were hands-on sessions with the computer to work with real data. The students were given several projects to work on during the week of school and they gave a short presentation at the Student's Seminar on the final day of the school. This was the first time that hands-on sessions were held during the X-ray school and it was a great success.

The students were very attentive and participated with great interest in the entire program. They attended the lectures, asked plenty of questions and as was clear from their final presentations,

FIGURE 34: Students during hands-on session.

worked hard on their projects and improved their understanding of X-ray data analysis. Many thanks to the instructors who worked on their lectures, the administration and computer groups for their support before and during the school, and to the computer specialists for their tremendous help at the hands-on sessions.

The school web page contains the details of the program and posts lectures on-line: http://xrayschool.gsfc.nasa.gov/docs/xrayschool/index.html.

email: xrayschool@milkyway.gsfc.nasa.gov

Aneta Siemiginowska

FIGURE 35: Keith Arnaud and Randall Smith working at their computers.

FIGURE 36: Maxim Markevitch during a discussion with the students. Kip Kuntz in the back helping students with their project.

FIGURE 37: Traditional reading of “Copenhagen”, the play by Michael Frayn.

FIGURE 38: A group photo on the final day of the school in front of Phillips Auditorium.

The Results of the Cycle 7 Peer Review

The Cycle 7 observing and research program was selected following the recommendations of the peer review panels. The peer review was held 21- 23 June 2005 at the Hilton Boston Logan Airport. 103 reviewers from all over the world attended the review, sitting on 13 panels to discuss 747 submitted proposals. The panels were organised as follows:

Galactic

Panels 1,2: Normal Stars, WD, Planetary Systems and Misc
Panels 3,4: SN, SNR + Isolated NS
Panels 5,6,7: WD Binaries + CVs, BH and NS Binaries, Galaxies: Populations

Extragalactic

Panels 8,9: Galaxies: Diffuse Emission, Clusters of Galaxies
Panels 10,11,12: AGN, Extragalactic Surveys

Big Project Panel: LP and VLP proposals

The over-subscription rate in terms of observing time for Cycle 7 was 6:1, very similar to previous cycles.

As is our standard procedure, all proposals were reviewed and graded by the topical panels, based primarily upon their scientific merit, across all proposal types. The topical panels produced a rank-ordered list along with detailed recommendations for individual proposals where relevant. The topical panels were allotted *Chandra* time to cover the allocation of time for GO observing proposals based upon the demand for time in that panel. They were also allocated money, similarly based upon demand, to fund archive and theory proposals. New this cycle, they were allotted a maximum number of constrained observations, based upon the number of constrained observations requested in that panel and chosen to ensure that only 15% of approved observations were time constrained. Large and Very Large Projects were discussed by the topical panels and ranked along with the rest, and the recommendations of these panels were recorded and passed to the Big Project Panel.

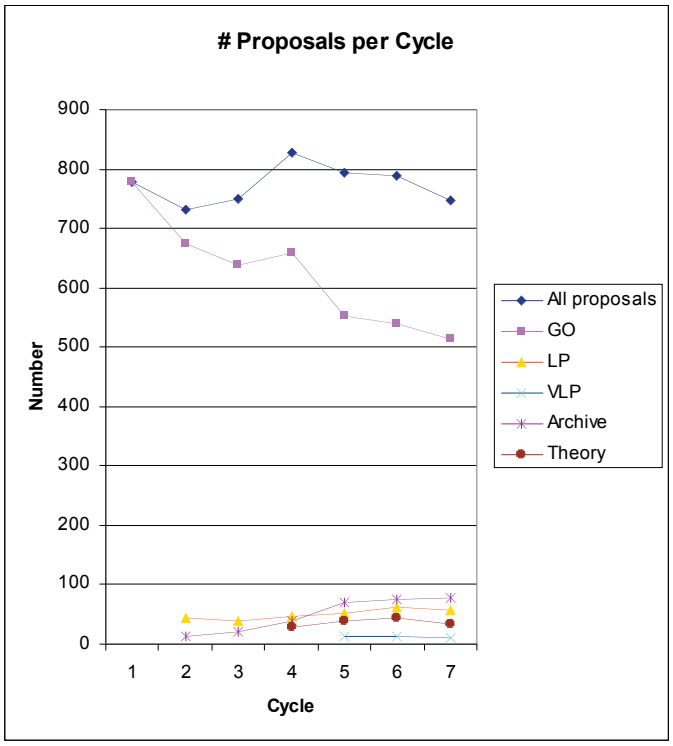

FIGURE 39: Proposals by type for each observing cycle.

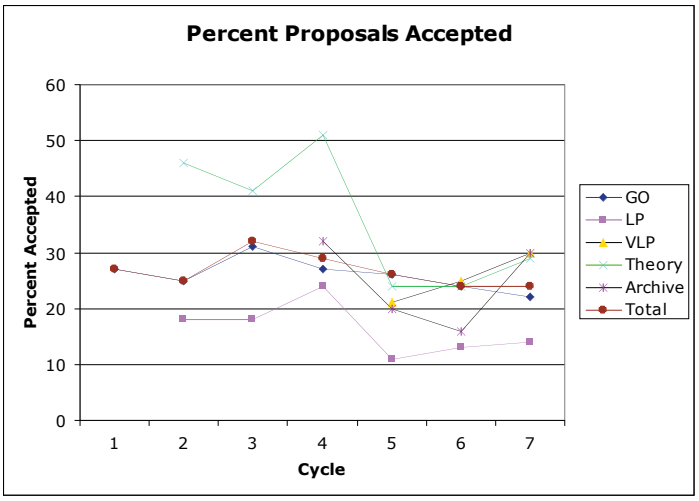

FIGURE 40: Percent proposals accepted by type, as a function of cycle.

Following the deliberations of these topical panels, the Big Project Panel discussed and recommended Large and Very Large Projects to be included in the Cycle 7 science program.

The resulting observing and research program for Cycle 7 was posted on the CXC website two weeks later, 8 July 2005. Letters detailing the results and providing a report from the peer review were mailed to each PI in early August. Observations of Cycle 7 targets began in the fall 2005, with an overlap of about 6 months expected before Cycle 6 observations are completed. This is an unusually long overlap due to the difficulty of scheduling observations with the restrictions on pitch angle in place in 2005.

Each year we publish numerical statistics on the results of the peer review These can be found from the "Statistics" link for a given cycle, which is linked from the "Target Lists and Schedules" area of our website. This year, for the first time, we are presenting a subset of those statistics here, in a more easily viewable form, based on presentations made to the *Chandra* Users' Committee. We expect this to become a regular feature in future Newsletters.

Figure 39 shows the number of proposals submitted of each proposal type (e.g. GO, LP, Archive etc.) as a function of cycle. Since more proposal types have become available in each cycle, the number classified as GO has decreased as other types increase.

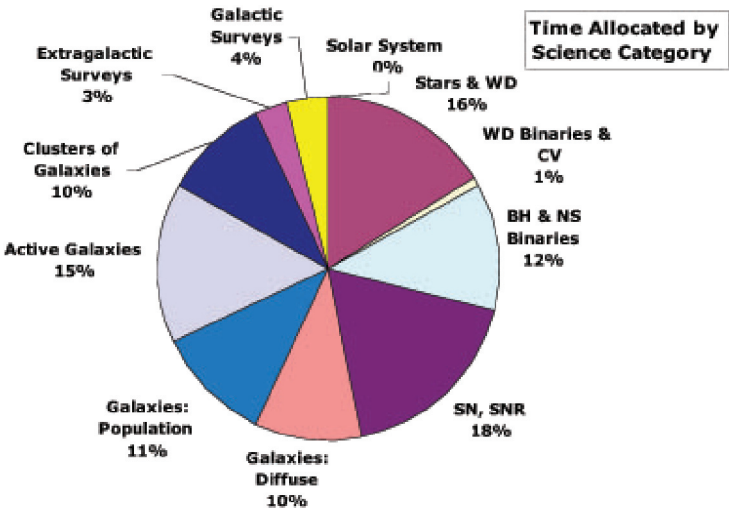

FIGURE 41: Time allocated by science category.

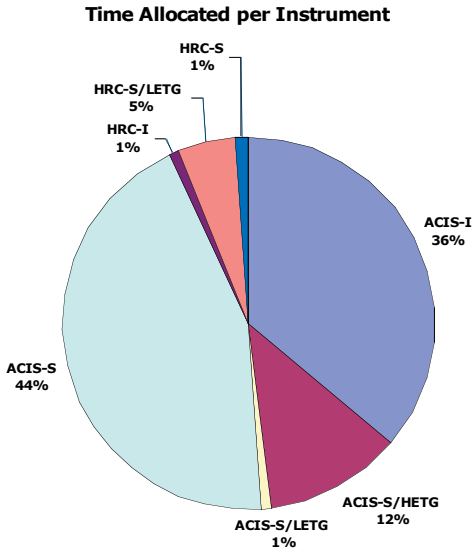

FIGURE 42: Time allocated by instrument.

The total number of submitted proposals is remarkably constant.

Figure 40 shows the percentage of proposals accepted, all or in part, for each type as a function of cycle. Please note that some of the fluctuations are due to small number statistics (e.g. Theory proposals).

Figure 41 is a pie chart indicating the percentage of *Chandra* time allocated in each science category. But note that the time available for each category is determined by the demand.

Figure 42, a second pie chart, shows the percentage of *Chandra* time allocated to observations for each instrument configuration.

Belinda Wilkes

Table 5 - Proposals by country.

Country	Submitted	Approved
Australia	2	
Austria	4	
Belgium	4	1
Brazil	2	
Canada	6	2
Finland	1	
France	8	3
Germany	22	8
Greece	1	
Israel	1	
Italy	28	7
Japan	18	2
Netherlands	21	8
Scotland	1	
Spain	5	2
Switzerland	6	3
United Kingdom	48	5
United States	569	142
Total Foreign	**178**	**41**

Chandra Fellows for 2006

This year we had a record number of applications for *Chandra* Postdoctoral Fellowships. The list of the Fellows for 2006 has just been finalized and is provided below.

Keep an eye on our web pages for information about the *Chandra* Fellows Symposium (October 2006) and the annual Fellowship competition (proposals due November, 2006).

Table 6 - List of accepted *Chandra* Fellows for 2006.

Name	PhD Institution	Host Institution
Carlos Badenes	Univ. Politcnica Catalunya	Rutgers
Shane Davis	UC Santa Barbara	Inst. Adv. Studies
Jifeng Liu	Univ. Michigan	CfA
Elena Rasia	Univ. Padova	Univ. Michigan
Masahiro Tsujimoto	Kyoto Univ.	Penn State

Nancy Remage Evans

Education & Public Outreach Proposals Selected In Cycle 7

The Cycle 7 Chandra EPO Peer Review, conducted by the CXC, was held in Cambridge MA on Dec. 7-9, 2005. A panel representing science, education, museum, Forum, and NASA mission and management perspectives reviewed 7 proposals. Four individual and 3 institutional proposals were submitted. Three individual and 2 institutional proposals were selected for funding. An overview of the selected proposals by type follows, alphabetically in order of PI last name.

Individual Proposals

Astrophysics Comes to Xavier University and Stays for Good

Science PI: Dr. Andrew Baker, NRAO
ajb@astro.umd.edu
Co-I: Dr. Shamibrata Chatterjee, NRAO
Education Co-I: Dr. Kathleen McCloud, Xavier University of Louisiana
Education Partner: Xavier University of Louisiana

Summary: This program plans to introduce NASA-related astronomy and astrophysics content to the physics program at Xavier University in New Orleans, a historically black college noteworthy for producing more African-American graduates with bachelor's degrees in physics than any other U.S. college or university. The physics curriculum currently lacks astronomy and astrophysics content. In collaboration with Dr. McCloud, who is Chair of the Xavier Physics Department, Drs. Baker and Chatterjee will work with the physics faculty on the development of appropriate astrophysics elements for existing physics courses, and with students on a hands-on instrumentation project. While the initial project is modest in scope, it is intended to produce a program with long-term sustainability.

Space Astronomy in the Schools: Astronomy Workshops for North Carolina Teachers

Science PI: Dr. Stephen Reynolds, North Carolina State University
steve_reynolds@ncsu.edu
Education Co-I: Dr. David Haase, The Science House/NCSU
Education Partner: The Science House (a statewide K-12 science/math outreach program based at NC State)

Summary: This program plans to provide workshops with astronomy content for two high need/low wealth school districts (Onslow and Cumberland County Schools) in southeastern North Carolina. Fifty teachers will be recruited to participate in training to increase their astronomy content knowledge and improve their use of inquiry-based teaching. Hands-on, inquiry-based activities will support the NC Science Standard Course of Study objectives. Teachers will be provided with materials as well as instruction to carry out the activities in their classrooms. The program will leverage the extensive expertise of the Science House staff in the delivery of such workshops.

Stop for Science! A Science Enrichment Program for Elementary Schools

Science PI: Dr. Patrick Slane, Harvard-Smithsonian Center for Astrophysics
pslane@cfa.harvard.edu
Education Partners: Fiske Elementary School, Lexington MA
Section Elementary School, Mukwanago WI

Summary: This program plans to develop materials aimed at science inquiry outside of the classroom to support the schools' formal efforts to improve science learning. The "Stop for Science" program will develop large format posters for display outside of the classroom that leverage the inherent interest of elementary age children in NASA and space-related content. The posters will use specific astronomy and space science-related examples to illustrate selected general science and math concepts drawn from grade-appropriate learning standards. The posters will be placed in non-classroom areas of the partner schools, accompanied by a series of inquiry-based questions that are used to stimulate the children to engage further with the poster content. The concept was previously piloted in the partner schools. This program will develop additional posters as well as teacher resource materials that tie the poster content to classroom science learning standards, and provide teachers with suggestions for related and extended topics, demonstrations, and activities.

Team Proposals

Chandra Astrophysics Institute (CAI)

Science PI: Dr. Frederick Baganoff, MIT
fkb@space.mit.edu
Education Co-I: Dr. Irene Porro, Kavli Inst., MIT
iporro@space.mit.edu
Education Partners: John D. O'Bryant (JDOB) School of Mathematics and Science, Boston MA
Rutgers Astrophysics Institute, Rutgers Univ.

Summary: This program will extend the CAI to the Boston Public Schools through a partnership with the newly established JDOB School, a specialized school within the Boston Public School system offering a comprehensive Science, Technology, Engineering, and Mathematics (STEM) curriculum to a diverse student population. The program will leverage resources from several NASA EPO initiatives to promote STEM learning and careers to underserved urban youth. CAI will offer a four-week intensive summer institute to prepare students and their teachers for school-year research projects in astrophysics using software developed by the Chandra EPO program and real data from the Chandra X-ray Observatory. The program will be carried out by the EPO staff of MIT's Kalvi Institute, and Chandra scientists,

with support from the Rutgers Astrophysics Institute. During the school year, the program will provide mentoring, weekly interactions with teachers and students by means of the Virtual Educational Space Resource, and review of student work in monthly meetings. In addition, students will participate in the After-School Astronomy Project which utilizes the resources of the Timothy Smith Network to provide after school enrichment and learning opportunities using the Universe Forum's Virtual Observing Network.

Rockets to Stars: Encouraging Girls' Interest in Astronomy and Technology

Science PI: Dr. Jennifer Sokoloski, Harvard-Smithsonian Center for Astrophysics
jsokoloski@cfa.harvard.edu
Education Co-I: Alejandra Pallais, Science Club for Girls
Education Partner: Science Club for Girls, Cambridge, MA

Summary: This program will provide NASA-related astronomy and technology content to the Science Club for Girls (SCFG), an after-school program whose goal is to keep girls engaged, confident and successful in science from kindergarten through high school by providing mentoring and leadership opportunties, affirming college as an expectation, and fostering careers in science and technology as goals and options. The PI, and three other CfA female astrophysicists, will work with the EPO Co-I to use existing NASA EPO materials to provide hands-on space science themed activities for middle school girls, and to enhance the learning experience of the club's all girl high school rocket team in the Team America Rocketry Challenge. The program will also provide NASA content training, role modeling, and leadership opportunities to club members who participate in the "Junior Assistant" program that provides peer mentoring to younger girls during family science nights and a summer science program.

Kathleen Lestition
Education and Public Outreach

HELPDESK

Questions can be sent to the CXC by using the HelpDesk facility. The HelpDesk is reached from a link on the header of the CXC web pages (i.e., at http://cxc.harvard.edu). The information entered into the form is passed into our HelpDesk Archive; we can easily track pending items with this tool. An introduction to the HelpDesk system is available from this same link.

Questions can also be sent to the HelpDesk staff using email (cxchelp@cfa.harvard.edu), but we prefer submissions through the web.

Constellation X-ray Mission Update

Science Highlights

The Constellation-X team rounded off the 2005 calendar year with several special sessions at Jan 06 AAS in Washington, DC. Nearly 300 people delayed their lunch on the first day of the meeting to attend a Con-X Town Hall meeting. In addition, 32 authors presented posters in special sessions 12 and 16, on Con-X technology development and example Con-X science. The hot handout at this AAS meeting was the Con-X Spectroscopy glasses: ``spectroscopy glasses for a spectroscopy mission''. Visitors to the Con-X booth went away with 1000 pairs of these glasses.

Con-X remains a high-priority NASA mission within the Beyond Einstein program; ranked 'next after JWST among major space missions' by the most recent Decadal Survey. The Decadal

FIGURE 43: Dr. Kim Weaver of GSFC (former Con-X Deputy Project Scientist) tries on the new Constellation-X spectroscopy glasses. The glasses contain a pair of transmittion diffraction gratings. Con-X will contain a set of x-ray reflection gratings optimized for low-energy spectroscopy. Mission Scientist Jay Bookbinder of SAO is on the right.

Survey priorities were re-affirmed by the 2005 NRC 'Mid Course Review'. Towards the end of 2005 Con-X and LISA took part in a GSFC-led Technology Assesment, which studied the technical readiness levels for key components to both missions. Con-X technologies continue to make good progress towards a launch in about 10 years, with the budget profile rather than technologies constraining the launch date.

In our report here one year ago we noted that the best slumped glass mirrors that have made were close to meeting the mission requirements without the baseline gold layer epoxied onto the reflecting surface. A substantial effort this year has been devoted to understand the limitations of this thermal slumping process, in order to identify ways to improve it. Studies to date indicate that one of the limitations may be errors in the figure of the

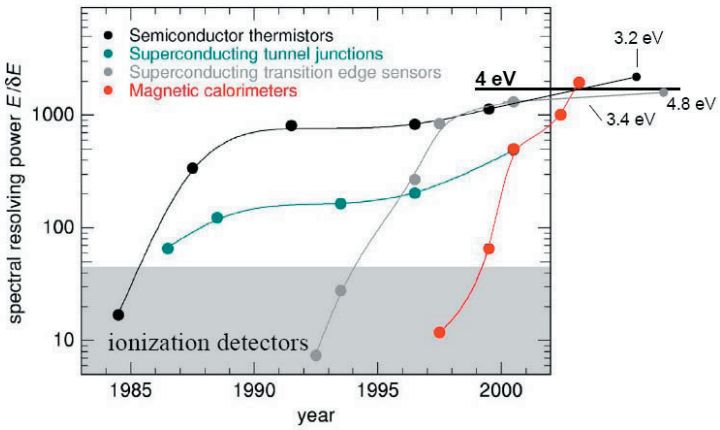

FIGURE 44: The energy resolution, expressed δE in eV, vs. time for a variety of classes of X-ray microcalorimeters. Several classes have already met the Con-X requirement of 4eV at 6keV. However, the δE is dependent on a large number of factors, and calorimeters with physical sizes and time constants appropriate for Con-X (ie, the transition edge sensors) have approached, but not yet met, the requirements. With the loss of the Suzaku calorimeter, the promise of non-dispersive high resolution X-ray spectroscopy will likely not be realized until Con-X.

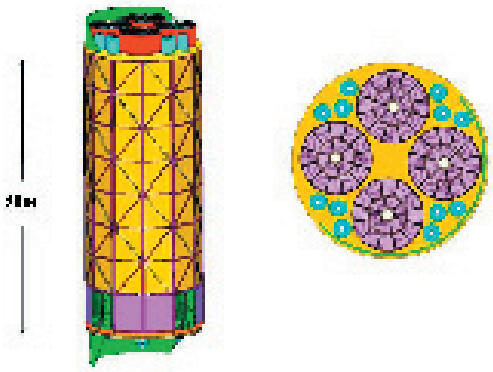

FIGURE 45: Side and top views of an alternative Con-X configuration which contains the same total number of telescopes (and effective area) at the baseline mission, but packs them all into a single spacecraft which could be launched on a Delta IVH vehicle. This configuration would save approximately $120m in launch costs.

slumping mandrel. However, reduction of these errors may allow only a modest improvement in the figure of the slumped glass. Understanding and improving the physics of the slumping process may be more important to the figure of the mirror segments.

Many separate groups have continued to make progress on the micro-calorimeter front. The best devices made to date have energy resolution better than the baseline mission requirements of 4eV at 6keV. However, these devices were not of the proper pixel size nor time resolution to be appropriate for use on Con-X. Devices with Con-X size and time parameters are approaching the required energy resolution, and improvements continue. Figure 44 shows a representative sample of micro-calorimeter energy resolution over time, showing the continuous improvements in energy resolution. The recent launch of Sukazu proved that micro-calorimeters can work in orbit, but also left the promise of the science they can yield unfullfilled.

Throughout 2005 a series of 15 workshops involving more than 60 scientists where held in order to examine the Con-X science case in light of the recent discoveries of Chandra and XMM. A brief summary of the conclusions is that the great imaging now being provided makes you thirst for high resolution spectroscopy even more! The workshops generated 15 white papers, containing over 100 pages of text, and were summarized in a May 2005 NASA technical publication titled 'Science with Constellation-X'. The white papers and science booklet are available on the Con-X web site, http://constellation.gsfc.nasa.gov.

While the science staff was busy with workshops and white papers, the engineering staff was studying alternative Con-X configurations which could meet or exceed the mission requirements and reduce cost and/or complexity. The new availability of the Delta-IVH launcher, which has higher lift capacity than the baselined Atlas-V, was one of the principal motivations for this study. Initial studies indicate that a single Delta-IVH launcher would save ~$120m in launch costs and carry the baseline 4 spectroscopy plus 12 high energy telescope configuration into orbit on a single spacecraft. Other configurations, consisting of 3, 2, or even a single telescope were considered but appear less suitable than this configuration. If subsequent studies prove its viability, this 4+12 telescope in one spacecraft configuration may become the new baseline. Figure 45 shows a cartoon drawing of this possible new configuration.

In closing, please join me in welcoming the new Con-X Instrument Scientists (IS) to the team: Jean Cottam is the Reflection Grating Spectrometer IS, Ann Parsons is the Hard X-ray Telescope IS, and Rick Shafer is the X-ray MicroCalorimeter Spectrometer IS.

Michael Garcia, for the Con-X team

SDS Under Martin Elvis

FIGURE 46: Martin Elvis.

Martin Elvis (Figure 46), who has led the Science Data Systems group since the AXAF science center came into existence in the early 1990s, has left the CXC to return to full time research as a member of SAO's High Energy Astrophysics Division. The SDS group is responsible for the scientific integrity of the *Chandra* data and data analysis software, and works closely with Pepi Fabbiano's Data Systems division which carries out the actual software development and pipeline and archive operations.

Martin brought to the *Chandra* team extensive experience in X-ray data analysis dating back to his days on the British Ariel 5 satellite team in the 1970s, when he made some of the first X-ray studies of Seyfert galaxies. Leading a group of scientists from SAO and MIT, Martin's vision for the SDS effort was to build a new generation of analysis tools which would be extensible, user-friendly and interoperable with other systems. Among the key ideas were multidimensionality - a design that would handle 1D, 2D and higher-dimensional data in the same way - and a non-axis-specific approach - tools that would apply the same algorithm to spectral, spatial, temporal and other axes. Another early idea was to build on the SAO team's experience with the IRAF-based PROS filtering and parameter interface, but make the individual tasks accessible from the operating system command line, making the system more open - an approach pursued at the same time by our colleagues at Goddard who were developing FTOOLS. SDS also build on MIT's intimate knowledge of the instruments and expertise with complex interactive data analysis software to create scientifically robust data products and an interactive environment.

The development of these ideas through preliminary and critical design reviews and interaction with the Data Systems division in the years before *Chandra* launch led to the systems we know today as CIAO and Standard Data Processing. During these years, Martin also led an active research group of postdocs and graduate students advancing multiwavelength studies of AGN.

After 11 years as one of Martin's SDS staff I took over leadership of the group in late 2004, and would like to express my appreciation of his stewardship during the key formative years of *Chandra* and CIAO.

- Jonathan McDowell

Supernova 1987A: Fast Forward to the Past

This article is taken from the Chandra Public Photo Album. Text and images can be found here:
http://chandra.harvard.edu/photo/2005/sn87a/index.html
- Editor

Recent *Chandra* observations have revealed new details about the fiery ring surrounding the stellar explosion that produced Supernova 1987A. The data give insight into the behavior of the doomed star in the years before it exploded, and indicate that the predicted spectacular brightening of the circumstellar ring has begun.

The supernova occurred in the Large Magellanic Cloud, a galaxy only 160,000 light years from Earth. The outburst was visible to the naked eye, and is the brightest known supernova in almost 400 years. The site of the explosion was traced to the location of a blue supergiant star called Sanduleak -69º 202 (SK -69 for short) that had a mass estimated at approximately 20 Suns.

Subsequent optical, ultraviolet and X-ray observations have enabled astronomers to piece together the following scenario for SK -69: about ten million years ago the star formed out of a dark, dense, cloud of dust and gas; roughly a million years ago, the star lost most of its outer layers in a slowly moving stellar wind that formed a vast cloud of gas around it; before the star exploded, a high-speed wind blowing off its hot surface carved out a cavity in the cool gas cloud (Figure 48).

The intense flash of ultraviolet light from the supernova illuminated the edge of this cavity to produce the bright ring seen by the Hubble Space Telescope (Figure 47). In the meantime the supernova explosion sent a shock wave rumbling through the cavity.

In 1999, *Chandra* imaged this shock wave, and astronomers have waited expectantly for the shock wave to hit the edge of the cavity, where it would encounter the much denser gas deposited by the red supergiant wind, and produce a dramatic increase in X-radiation. The latest data from *Chandra* and the Hubble Space Telescope indicate that this much-anticipated event has begun.

Optical hot-spots now encircle the ring like a necklace of incandescent diamonds (Figure 49, top back cover). The *Chandra* image (see Figure 50, back cover) reveals multimillion-degree gas at the location of the optical hot-spots.

X-ray spectra obtained with *Chandra* provide evidence that the optical hot-spots and the X-ray producing gas are due to a collision of the outward-moving supernova shock wave with dense fingers of cool gas protruding inward from the circumstellar ring (see illustration; Figure 48). These fingers were produced long ago by the interaction of the high-speed wind with the dense circumstellar cloud.

The dense fingers and the visible circumstellar ring represent only the inner edge of a much greater, unknown amount of matter ejected long ago by SK -69. As the shock wave moves into the dense cloud, ultraviolet and X-radiation from the shock wave will heat much more of the circumstellar gas.

Then, as remarked by Richard McCray, one of the scientists involved in the *Chandra* research, “Supernova 1987A will be illuminating its own past.”

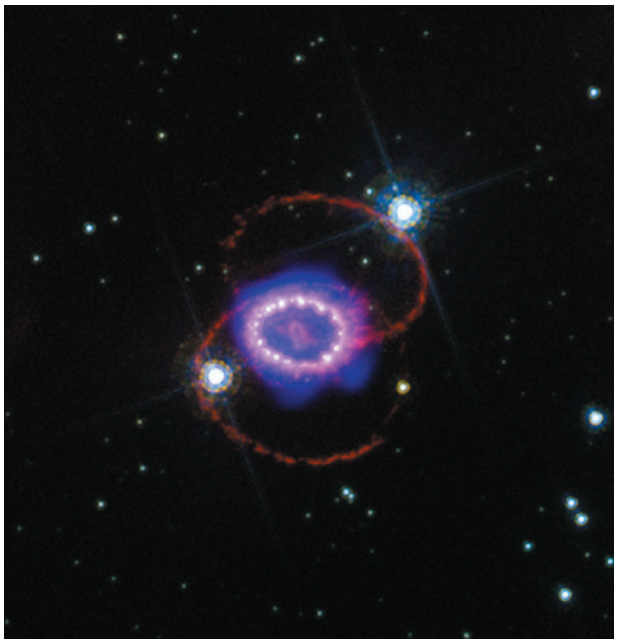

FIGURE 47: *Chandra* X-ray (blue) and Hubble optical (red) composite of Supernova 1987A. Credit: X-ray: NASA/CXC/PSU/S. Park & D. Burrows; optical: NASA/STScI/CfA/P. Challis.

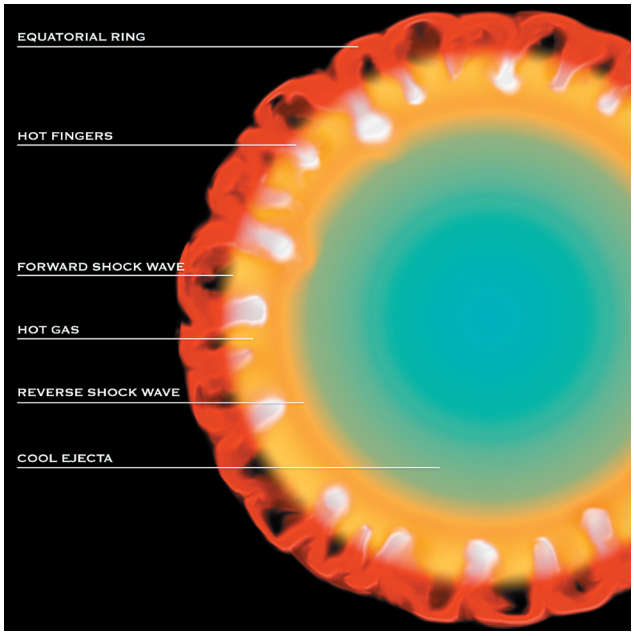

FIGURE 48: Schematic illustration of Supernova 1987A dynamics. Credit: NASA/CXC/M. Weiss.

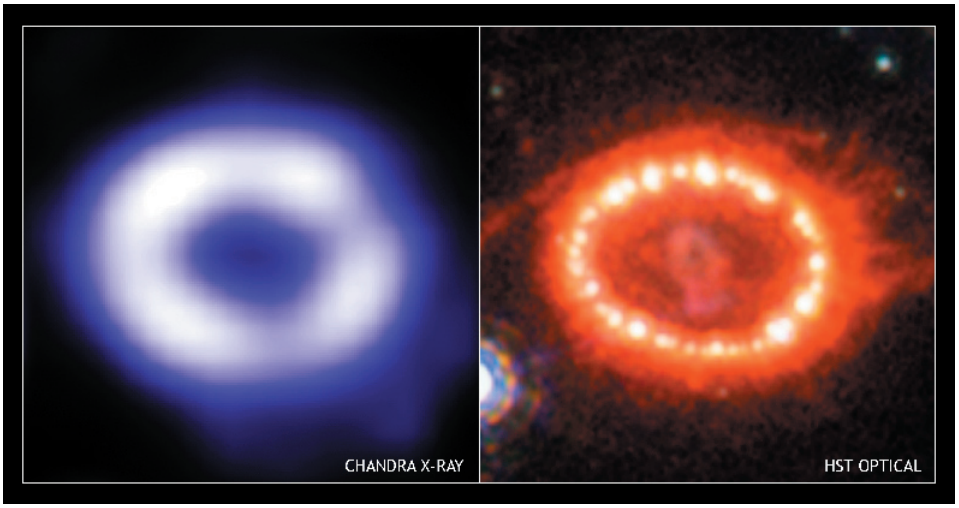

FIGURE 49: Chandra and HST images of SN 1987A. Credit: X-ray: NASA/CXC/PSU/S. Park & D. Burrows; optical: NASA/STScI/CfA/P. Challis.

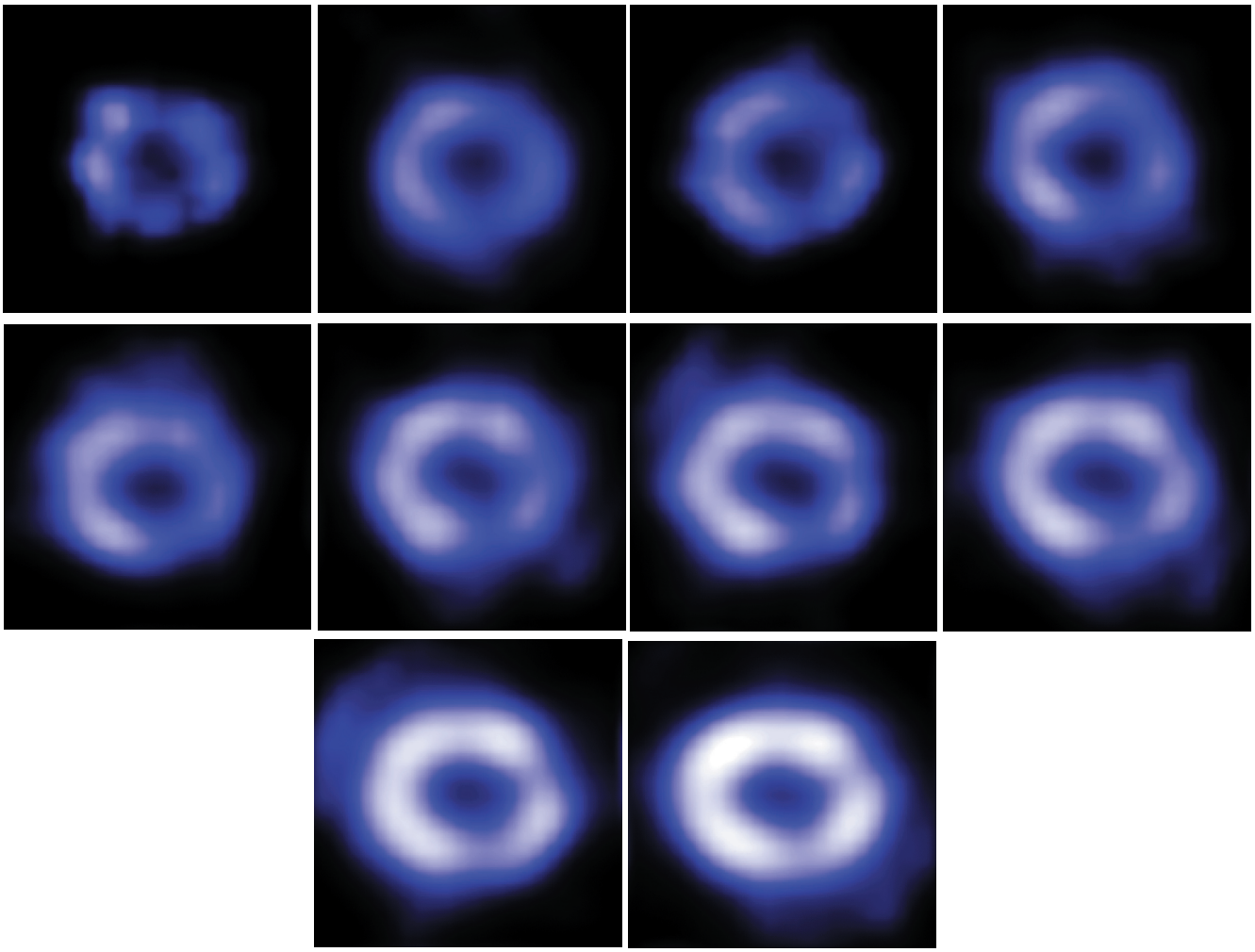

FIGURE 50: These X-ray images of Supernova 1987A were taken between January 17, 2000 and January 09, 2005. *Chandra* observations have revealed new details about the fiery ring surrounding the stellar explosion that produced Supernova 1987A. The data give insight into the behavior of the doomed star in the years before it exploded, and indicate that the predicted spectacular brightening of the circumstellar ring has begun. Credit: NASA/CXC/PSU/S. Park & D. Burrows. **(See article on page 47)**

The *Chandra* Newsletter currently appears approximately once a year. We welcome contributions from readers. Nancy Remage Evans edits "*Chandra* News", with assistance from Samantha Stevenson. Comments on the newsletter and corrections and additions to the hardcopy mailing list should be sent to: chandranews@cxc.harvard.edu.